SOVIET PHYSICS USPEKHI VOLUME 10, NUMBER 4 JANUARY-FEBRUARY 1968

539.17.01

SOME PROBLEMS IN THE THEORY OF NUCLEAR REACTIONS AT HIGH ENERGIES

I. S. SHAPIRO

Usp. Fiz. Nauk 92, 549—582 (August, 1967)

I. INTRODUCTION

AT present it is customary to divide nuclear reactions into two classes: a) processes in which the energy and the momentum of the incident particle are distributed over many degrees of freedom of the nucleus and b) direct reactions, which are distinguished by the transfer of the energy and the momentum primarily to a single nucleon or to a comparatively small group of nucleons (deuteron, triton, alpha-particle etc.).

At low and medium energies the processes of the first type reduce essentially to the formation and decay of compound nuclei. At high energies in reactions of this type a large number of particles is observed to be emitted which are either weakly or not at all correlated (in the c.m. system for the reaction) with the direction of motion of the incident particle.

On the other hand direct processes are characterized by the emission of one or several particles which carry away practically completely the energy and the momentum imparted to the nucleus. In such a case a small amount of momentum and, as a rule, a very small amount of energy is transferred to the residual nucleus (frequently the nucleus remains in the ground state or a state of low excitation). The angular distributions of particles emitted in direct processes are sharply anisotropic and have only a weak dependence on the energy of the initial particles.

Possible Approaches to the Theory of Nuclear Reactions at High Energies

With respect to the reactions in which a large fraction of the energy and the momentum of the incident particle is transferred to the main part of the nucleus the theory is at the stage of very rough models. They may be subdivided into three groups: the simple statistical model, thermodynamic models, the cascade mechanism.

The simple statistical model involves the assumption of the slowness of variation of the reaction amplitude compared to the phase space (the consequences arising from such an assumption are explained below; cf., pp. 00—00). The validity of the basic assumption in this model is limited by the existence of quasistationary states of nuclei which decay with the emission of nucleons or of compound particles. In the case of light nuclei and not very high degrees of excitation this means that the reaction amplitude varies as a function of the relative energy of a pair of final particles in a resonance manner. But if the energy of excitation of the residual nuclei is sufficiently high so that the probability for their decay is determined by the density of levels of the final nucleus, then the spectrum of the final particles will be of the evaporation type.

The essence of the thermodynamic models consists of the assumption that the nuclear reaction proceeds in two stages: at first the energy of the colliding particles is redistributed between the degrees of freedom of the system under consideration (i.e., thermodynamic equilibrium is established), and then the system begins to disintegrate (to cool off). As is well known, at low energies of the colliding particles the formation of the compound nucleus does in fact take place, and this fact can be easily interpreted, since the widths of the excited nuclear levels are sufficiently small (i.e., the lifetime of the compound nucleus is much greater than a characteristic nuclear time). But with an increase in the excitation energy the partial widths of the levels also increase. Moreover, it appears probable that although the number of quasistationary levels is great, it is still finite (in analogy with the bound states of a particle in a potential well). Therefore, the possibility of formation of an equilibrium compound system at high energies becomes doubtful. Under such circumstances a theoretical discussion of specific phenomena becomes highly speculative and difficult to check by experiment, since the thermodynamic considerations in nuclear physics often turn out to be on the borderline of applicability owing to the relatively small number of systems in the statistical ensemble and to the important role played by fluctuations as a result of this.

The idea of the intranuclear cascade processes (usually calculated by means of the Monte Carlo method) consists of the nucleus being regarded as a set of free independent nucleons with one of which the incident particle collides. The nucleon which acquires the momentum and the energy (or, in other words, the secondary particle) collides with other nucleons etc. The predictions of the cascade model lack pronounced qualitative characteristics, in other words they are not unique, and, therefore, there is never any certainty that even those experimental data that agree with this model could not be explained in a different manner. This circumstance is of considerable importance if we take into account the fact that the cascade model has a rather poor physical basis: an examination of the simplest examples convinces one of the necessity of taking into account the relative motion of the nucleons

and the structure of the nucleus even at high energies.

To a large extent, for the reasons indicated above, the theory of processes involving large transfers of energy and momentum to the nucleus will not be considered in this article. However, this does not mean that we consider that an empirical study of such phenomena is not worthy of attention. Perhaps it may be this very region that will bring surprises which are by no means infrequent in the history of nuclear physics.

Current ideas on the nature of direct processes reduce, in short, to the assumption that a reaction of such type is the result of the collision of the incident particle with some virtual particle (nucleon, deuteron, alpha-particle etc.) emitted by the target nucleus for a short period of time. A quantitative formulation of this kind of concept leads to the formalism of Feynman diagrams (the well known impulse approximation, in particular, corresponds to the simplest of such diagrams). The application of this method to the theory of direct reactions brought about by high energy particles constitutes the object of the present review.

In this first section the necessary general information and definitions are given. Section II is devoted to a brief presentation of the essence and of the physical content of the method of Feynman diagrams. In Secs. III and IV pole diagrams are investigated (attention is primarily directed to the methods of identifying the pole mechanism and to pointing out the experiments required to achieve this aim). In the last section V the so-called final state interaction is considered (i.e., processes of the "rescattering" by the residual nucleus of the products of a virtual reaction). We are also here pursuing the goal of making manifest such observed effects which would enable one to establish the mechanism of the process (i.e., the number and the kinds of virtual particles and virtual reactions).

What is Achieved by Utilizing High Energy Particles for Studying Nuclei?

In nuclear physics it is customary to say that the energy introduced into a nucleus by some external agency is high if it is considerably in excess of the average binding energy per nucleon in the nucleus (6—9 MeV). Thus, in order of magnitude the high energy region begins from 100 MeV.

It is possible to study nuclear reactions at high energies with two aims in mind: to investigate the properties of the nucleus itself or to obtain information on the interaction between elementary particles and nucleons. In the former case the question naturally arises: what new information can be provided by utilizing high-energy particles? Here one must first of all point to three circumstances.

The first of these consists simply of the fact that as the energy of the incident particles is increased the range is extended of the values of the kinematic variables allowed by the conservation laws and by the relationship between the energy and the momentum of the free particle (the so called physical region).

A second less trivial circumstance is that the existence of nucleon isobars and of the associated resonance energy dependence of the amplitudes for the scattering of mesons by nucleons can under certain conditions be utilized for identifying the virtual processes constituting the mechanism of the reaction.

Finally, a third specific source of information are the reactions of meson capture and of double charge exchange of pions. These reactions can enrich our information concerning reduced widths for deuterons, tritons, α particles etc., or, in other words, concerning the structure of the "cloud" of virtual particles surrounding the nucleus.

It is necessary to emphasize that even at very high energies nuclear structure can affect the course of direct nuclear reactions in an essential manner. The cross sections for reactions of this type at high energies will contain the same constants (reduced widths) as in the case of low energies. An independent determination of these constants from experiments at low and at high energies must give consistent results if our ideas regarding the mechanism of direct processes are correct.

The possibility of a unified description, in the sense indicated above, of direct nuclear reactions over a broad range of energies is significant also in the case when for one reason or another the nucleus is utilized merely as a target containing nucleons. Indeed, in order to determine on the basis of an experimentally measured nuclear cross section the unknown characteristics of an elementary event (i.e., the interaction of the incident particle with the nucleon) it is necessary to obtain in an independent manner information concerning the mechanism of the reaction and the constants determined by the nuclear structure.

Amplitude, Cross Section, Phase Space

The amplitude for the reaction

$$1+2\rightarrow 3+4+\ldots+n \tag{1.1}$$

is the term applied to the complex quantity $M_{\beta\alpha}$ related to the differential cross section $d\sigma_{\beta\alpha}$ by the equation

$$d\sigma_{\beta\alpha}=\frac{1}{v_{12}}\frac{|\mu_{\beta\alpha}|^2}{(2\pi)^{3n-10}}\delta(P_i-P_f)\,d^3p_3\,d^3p_4\ldots d^3p_n, \tag{1.2}$$

$$v_{12}=\sqrt{(\mathbf{v}_1-\mathbf{v}_2)^2-[\mathbf{v}_1\mathbf{v}_2]^2}. \tag{1.3}$$

Here the indices α and β denote the discrete quantum numbers of the initial and final states, P_i and P_f are the total four-momenta of these states, p_1, p_2, ..., p_n are the momenta of the particles participating in the reaction, v_1 and v_2 are the velocities of particles 1 and 2. In formulas (1.2), (1.3), and everywhere in subse-

quent discussion we shall assume $\hbar = c = 1$ unless explicitly stated otherwise. The quantity v_{12} is numerically equal to the flux density j_0 under the condition that one pair of colliding particles is present per unit volume.

The probability of the reaction $d\omega_{\beta\alpha}$ is related to the differential cross section by the equation

$$d\sigma_{\beta\alpha} = \frac{d\omega_{\beta\alpha}}{j_0 \Delta t}, \tag{1.4}$$

where Δt is the duration of the observation. This means that the reaction probability per unit time $d\lambda_{\beta\alpha}$ is determined by the expression

$$d\lambda_{\beta\alpha} = \frac{d\omega_{\beta\alpha}}{\Delta t} = v_{12}\, d\sigma_{\beta\alpha}, \tag{1.5}$$

where $d\sigma_{\beta\alpha}$ is given by formula (1.2).

The final aim of the study of every nuclear reaction is the establishment of the functional dependence of the amplitude on the kinematic variables—the momenta and the energies of the initial and the final particles.

The number of independent kinematic variables is determined by the number of particles participating in the reaction, by the conservation laws, by the relation between the energy and the momentum for a free particle and by the invariance of the amplitude under rotations and Lorentz transformations (or Galilean transformations if all the particles are nonrelativistic).

If the amplitude does not depend on the spin states of the particles before and after the reaction then all the kinematic variables must be invariants of the transformations of the coordinate systems and the total number of such independent invariant variables is equal to $3n - 10$, where n is the total number of particles participating in the reaction (it is assumed that $n \geq 4$). We note that in addition to the invariant functions the amplitude also contains the factor $(2\mathscr{E}_1 \cdot 2\mathscr{E}_2 \ldots 2\mathscr{E}_n)^{-1/2}$ where $\mathscr{E}_n$ are the total energies of the particles participating in the reaction. The invariant variables can be chosen in different ways. For example, for $n = 4$ (two particles in the final state) their number is equal to 2, and they can be chosen in the following manner:

$$s_{12} = (P_1 + P_2)^2, \quad t_{13} = (P_1 - P_3)^2. \tag{1.6}$$

Here P are the four-momenta of the particles, with

$$p^2 \equiv \mathscr{E}^2 - \mathbf{p}^2, \tag{1.7}$$

where $\mathscr{E}$ is the total energy of the particle.

We note that in virtue of the conservation laws we have

$$s_{12} = s_{34}, \quad t_{13} = t_{24}. \tag{1.8}$$

As may be easily seen, s_{12} is the square of the total energy of particles 1 and 2 in their center of mass system, while t_{13} determines the square of the transferred momentum. Moreover, one could also utilize the variable $t_{23} = t_{14}$:

$$t_{23} = (p_2 - p_3)^2. \tag{1.9}$$

But between s_{12}, t_{13}, and t_{23} there exists the linear relation

$$s_{12} + t_{13} + t_{23} = m_1^2 + m_2^2 + m_3^2 + m_4^2, \tag{1.10}$$

where m are the masses of the particles.

As pointed out previously, the term "high energy particle" in nuclear physics does not exclude the possibility that the particle can be nonrelativistic. In such a case instead of s_{12}, t_{13} or t_{23} it is convenient to utilize the variables $\bar{s}_{12}$, $\bar{t}_{13}$ or $\bar{t}_{23}$ which are invariant with respect to Galilean transformations and rotations:

$$\bar{s}_{12} = -(\mathbf{p}_1 + \mathbf{p}_2)^2 + 2(m_1 + m_2)(E_1 + E_2), \tag{1.11}$$

$$\bar{t}_{13} = -(\mathbf{p}_1 - \mathbf{p}_3)^2 + 2(m_1 - m_3)(E_1 - E_3), \tag{1.12}$$

$$\bar{t}_{23} = -(\mathbf{p}_2 - \mathbf{p}_3)^2 + 2(m_2 - m_3)(E_2 - E_3). \tag{1.13}$$

Here

$$E = \frac{p^2}{2m} \tag{1.14}$$

is the kinetic energy of the nonrelativistic particle. Up to terms of order E^2/m^2 we have

$$\bar{s}_{12} = s_{12} - (m_1 + m_2)^2, \quad \bar{t}_{13} = t_{13} - (m_1 - m_3)^2,$$

$$\bar{t}_{23} = t_{23} - (m_2 - m_3)^2. \tag{1.15}$$

From (1.8) and (1.15) it follows that

$$\bar{s}_{12} + \bar{t}_{13} + \bar{t}_{23} = -2m_4 Q, \tag{1.16}$$

where

$$Q = m_1 + m_2 - m_3 - m_4. \tag{1.17}$$

We note that

$$\left.\begin{aligned} \bar{s}_{12} &= \bar{s}_{34} - 2(m_3 + m_4)\, Q, \\ \bar{t}_{13} &= \bar{t}_{24} - 2(m_2 + m_4 - m_1 - m_3)\, Q, \\ \bar{t}_{23} &= \bar{t}_{14} - 2(m_1 + m_4 - m_2 - m_3)\, Q. \end{aligned}\right\} \tag{1.18}$$

It is also clear that $\bar{s}_{ij}/2(m_i + m_j)$ is the kinetic energy of the particles i and j in their center of mass system.

If reactions involving production of three particles are being considered, then $n = 5$ and the number of invariant variables will be $3 \times 5 - 10 = 5$. In this case one can select as independent variables, for example

$$s_{12},\ s_{34},\ s_{45},\ t_{13},\ t_{24} \tag{1.19}$$

or the corresponding nonrelativistic variables.

When the reaction amplitude depends on the spin states of the particles then it contains invariants formed from spin-tensors and momenta. The coefficients associated with these invariants are functions of the invariant variables and are referred to as invariant amplitudes. They determine the complete dynamics of the process (or, in other words, the mechanism of the reaction) since the construction of the

spin-tensors themselves is a purely kinematic problem the solution of which can be carried through to the end if the spins of the particles are known.

The number of invariant amplitudes determining the number of independent experiments required for a complete reconstruction of the amplitude from the experimental data is generally speaking, equal to

$$(2J_1+1)(2J_2+1)\times\ldots\times(2J_n+1), \qquad (1.20)$$

where J are the spins of the particles. In the n = 4 case the conservation of parity reduces this number by approximately a factor of two.

The increase in the number of invariant variables and of invariant amplitudes with increasing n is the first reason why the study of nuclear reactions with the emission of a large number of nucleons becomes extraordinarily complicated. Indeed, in this case it is necessary either to test experimentally the theoretical predictions concerning the behavior of several functions of a large number of variables, or, if there exists no quantitative theory of the phenomenon, to reconstruct these functions from the experimental data. In the present state of nuclear experiments it is hardly possible to achieve either one of these two objects. The second circumstance preventing the elucidation of the mechanism of the reaction in the case of large n (practically for n > 5) is the fact that in this case the so-called phase space often turns out to be a much more rapidly varying function of the kinematic variables than the amplitude itself.

The phase space ΔV is usually the term used to denote the integral

$$\Delta V=\int_G \delta(P_i-P_f)\,d^3p_3\,d^3p_4\ldots d^3p_n. \qquad (1.21)$$

The domain of integration G in (1.21) corresponds to the given ranges of variation of the momenta of the final particles. It is clear that if $|M_{\beta\alpha}|^2$ is a function of the kinematic variables which varies much more slowly than the phase space ΔV, then it is the latter that will in the main determine the variation of the differential cross section (1.2). If G encompasses the whole range of variation of the momenta p_3, p_4, ..., p_n determined by the conservation laws, then formula (1.21) gives the total phase space of the reaction V which for sufficiently large n will significantly affect the dependence of the total cross section for the reaction on the energy of the colliding particles.

The integration in (1.21) for arbitrary n can be carried out only numerically. However, in the nonrelativistic limit the integral (1.21) can be evaluated analytically. In this approximation we have for the total phase space

$$V=\frac{(2\pi)^{3(l-1)/2}}{\Gamma\left(\frac{3l-3}{2}\right)}\,m_{34\ldots n}^{3/2}W^{\frac{3l-5}{2}}, \quad l=n-2, \qquad (1.22)$$

where

$$m_{34\ldots n}=\frac{m_3m_4\ldots m_n}{m_3+m_4+\ldots+m_n}, \qquad (1.23)$$

$$W=Q+E_1+E_2=E_3+E_4+\ldots+E_n \qquad (1.24)$$

(W is the total kinetic energy of the final particles in their center of mass system) and

$$\Gamma\left(\frac{3l-3}{2}\right)=\begin{cases}\left(\frac{3l-5}{2}\right)!, & \text{if } l \text{ is odd}\\ 2^{\frac{4-3l}{2}}\sqrt{\pi}(3l-5)!!, & \text{if } l \text{ is even.}\end{cases} \qquad (A)$$

Remaining within the framework of the nonrelativistic approximation it is not difficult to obtain also the dependence of the differential cross section on the kinematic variables as determined by the phase space. For example, for the energy spectrum of one of the final particles we obtain, setting $|M_{\beta\alpha}|^2 = \text{const}$

$$\frac{d\sigma_{\beta\alpha}}{dE_3}=C\sqrt{\frac{E_3}{W}}\left(1-\frac{m_3+m'}{m'}\,\frac{E_3}{W}\right)^{\frac{3n-14}{2}}. \qquad (1.25)$$

Here

$$m'=m_4+m_5+\ldots+m_n, \qquad (1.26)$$

$$C=\frac{\sigma_{\beta\alpha}}{W}\sqrt{\frac{\pi}{2}}\left(\frac{m_3\cdot m_{45\ldots n}}{m_{34\ldots n}}\right)^{3/2}\frac{\Gamma\left(\frac{3n-9}{2}\right)}{\left(\frac{3n-12}{2}\right)}, \quad n>4, \qquad (1.27)$$

where $\sigma_{\beta\alpha}$ is the total cross section.

For the angular correlation between two of the final particles (for example, 3 and 4) we have

$$\frac{d\sigma_{\beta\alpha}}{dz}=\sigma_{\beta\alpha}\left(\frac{m''m_{56\ldots n}}{m_{34\ldots n}}\right)^{3/2}\varphi(z), \qquad (1.28)$$

where z is the cosine of the angle between the momenta of particles 3 and 4 in the center of mass system for the reaction,

$$\varphi(z)=\frac{a^2}{\pi(1-az^2)^2}\left[\frac{1+2az^2}{\sqrt{a(1-az^2)}}\left(\frac{\pi}{2}-\operatorname{arctg} z\sqrt{\frac{a}{1-az^2}}\right)-3z\right], \qquad (1.29)$$

$$m''=m_5+m_6+\ldots+m_n, \qquad a=\frac{m_3m_4}{(m_3+m'')(m_4+m'')}. \qquad (1.30)$$

If m'' is considerably larger then the mass of either one of the particles 3 or 4, then $a \ll 1$ and formula (1.29) becomes considerably simplified:

$$\varphi(z)\approx\frac{a^{3/2}}{2}\left(1-\frac{8}{\pi}\sqrt{a}z\right). \qquad (1.31)$$

From the formulas given above it follows that the dependence on the kinematic variables determined only by the phase space alone can be quite sharp. This can be illustrated by several examples.

Figures 1, 2, and 3 respectively show the spectra for protons, deuterons, and tritons produced in the capture by the C^{12} nucleus of stopped π^- mesons. The dotted curves calculated by means of formulas (1.25)—(1.27) correspond to energy spectra determined by the phase spaces for the reactions

$$C^{12}+\pi^-\rightarrow\begin{cases}Be^8+p+3n,\\ Be^8+d+2n,\\ Be^8+t+n.\end{cases} \qquad (1.32)$$

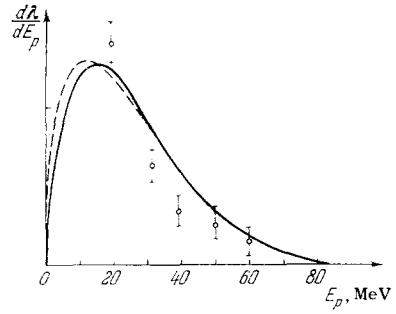

FIG. 1. The energy spectrum of the protons in the reaction $C^{12} + \pi^- \to Be^8 + p + 3n$. Dotted curve – phase space, solid curve – α-particle mechanism.

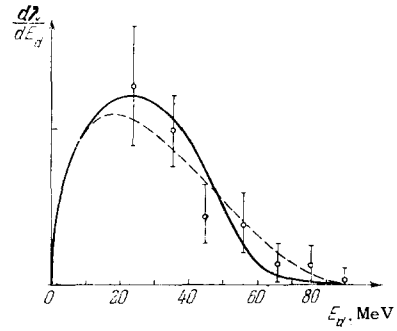

FIG. 2. The energy spectrum of the deuterons in the reaction $C^{12} + \pi^- \to Be^8 + d + 2n$. Dotted curve – phase space, solid curve – α-particle mechanism.

The solid curves are obtained under the assumption that the mechanism of the reactions (1.32) reduces to the emission by the C^{12} nucleus of a virtual α particle which captures a π^- meson. In this case the amplitude for the reaction depends on the momentum distribution of the virtual α particles which at sufficiently low momenta of the residual Be^8 nucleus is wholly determined by the effective range of the forces between an α particle and the Be^8 nucleus and by the energy required to separate the α particle from the Be^8 nucleus. As can be seen from Figs. 1 and 2, the dependence determined by the phase space turns out to be so strong that taking into account the available accuracy it is not possible to make any conclusions regarding the mechanism of the reaction based on the experimental data on the energy spectra of the protons and deuterons.

A completely different situation exists in the case of the energy spectrum of tritons (Fig. 3). In this case the number of final particles is smaller and the phase space turns out to be a much smoother function which significantly differs from the shape of the curve for differential cross section evaluated on the assumption of the "α-particle mechanism" for the capture of π^- mesons (the theoretical curves in Figs. 1–3 have been taken from the article by Kolybasov[1], and the experimental data from the paper by Vaĭsenberg and co-workers[2]; cf., also[3]).

Figure 4 shows the angular correlation between two

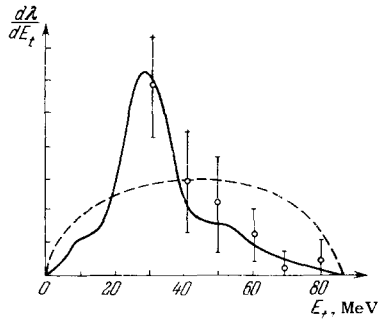

FIG. 3. The energy spectra of the tritons in the reaction $C^{12} + \pi^- \to Be^8 + t + n$. Dotted curve – phase space, solid curve – α-particle mechanism.

neutrons produced in the first two reactions (1.32). The dotted curve is calculated by means of formulas (1.28)–(1.30) for the capture of a π^- meson by a free α particle at rest, i.e., it is entirely determined by the phase space of the reactions

$$He^4 + \pi^- \to \begin{cases} p + 3n, \\ d + 2n. \end{cases} \qquad (1.33)$$

The fact that both reactions (1.33) are described by a single curve is explained by the structure of the function $\varphi(z)$ which depends only on the masses of particles 3 and 4 and the total mass of all the remaining particles. The solid curve 1 corresponds to the "α-particle mechanism" for the capture of a π^- meson mentioned above. For comparison Fig. 4 also shows experimental data of Ozaki et al.[4], which are interpreted by some authors (cf., for example,[5,6]) as a confirmation of the two-nucleon mechanism for pion absorption (in Fig. 4 curve 2 corresponds to such a "deuteron mechanism"; all the theoretical curves in this diagram are

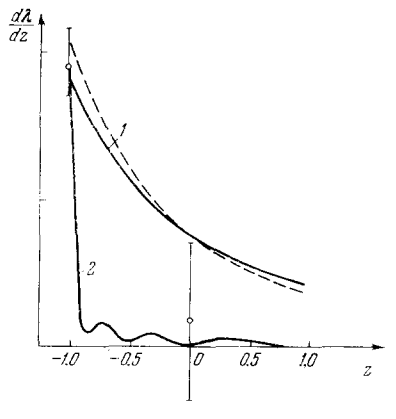

FIG. 4. Angular correlation of neutrons formed in the reactions

$$C^{12} + \pi^- \to \begin{cases} Be^8 + p + 3n, \\ Be^8 + d + 2n. \end{cases}$$

Dotted curve – phase space for the reactions

$$\pi^- + He^4 \to p + 3n, \quad d + 2n.$$

Solid curve 1 – α-particle mechanism, curve 2 – deuteron mechanism.

taken from the paper by Kolybasov[7]). As can be seen from Fig. 4, at present one can hardly draw such a conclusion with certainty, and for the solution of this problem it is necessary to decrease the experimental error by at least a factor of two (we note that a number of other facts also provide ground for doubting the dominant contribution of the two-nculeon mechanism of pion absorption by C^{12} and O^{16} nuclei (cf.[1-3])).

II. FEYNMAN DIAGRAMS

Amplitudes Instead of Wave Functions

The method of Feynman diagrams differs from the well-known Schrödinger formalism by the fact that it enables us to avoid the explicit use of nuclear wave functions. This latter fact is essential particularly in the case when we consider direct reactions with the emission of nuclear particles more complicated than nucleons, or when such particles occur in the intermediate stages of the reaction in virtual form (for example, in the reactions of meson capture, double charge exchange of pions, and others). Indeed, the nucleus can almost never be regarded as a stationary system of deuterons, tritons, α particles, etc. since the distance between the "internal levels" for each of these particles can not be regarded as large compared to the nuclear levels. In terms of classical physics this means that the motion of the center of mass of a particle in the nucleus is not slow compared to the motion of nucleons within the particle itself. In other words, the individuality of the compound particles in the nucleus is lost or, more exactly, their number is not conserved: they are formed and dissociate with a period equal in order of magnitude to the duration of a direct reaction (i.e., to the time of passage of a fast particle through the nucleus). Insofar as the wave function for the nucleus cannot be represented in the form of a product of "internal" wave functions of the particles and a wave function describing their relative motion, the reactions involving compound particles (real or virtual' have a different appearance in the Schrödinger formalism than reactions in which only nucleons participate. This circumstance does not correspond to the experimental facts according to which no qualitative difference is observed between direct reactions involving the emission of nucleons or of compound particles. Such a "nonequivalence" of compound particles and of nucleons does not occur in the method of Feynman diagrams, in which any nucleus appears in the theory on the same basis as an elementary particle.

In the diagram method the basic concept of the theory is not a wave function, but an amplitude of a real or a virtual process. Moreover, the real and the virtual processes are described by the same amplitude but only corresponding to different values of the kinematic variables.

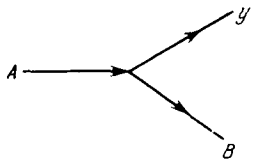

FIG. 5. Diagram for the decay A → B + y.

Amplitude of the Virtual Process

We consider the decay

$$A \to B + y \tag{2.1}$$

of the nucleus A into the nucleus B and the particle y which we represent by the diagram shown in Fig. 5.

If the decay is actually possible, then as a consequence of the conservation laws and of the relations between the energy and the momentum for each of the particles all the kinematic variables are fixed and are determined by the masses of the particles. Specifically, the momenta p_B, p_y of the nonrelativistic particles B and y in their center of mass system are determined by the equations

$$\mathbf{p}_B = -\mathbf{p}_y = \mathbf{q}, \tag{2.2}$$

$$q^2 = 2m_{By}Q, \quad Q = m_A - m_B - m_y, \quad m_{By} = \frac{m_B m_y}{m_B + m_y}, \tag{2.3}$$

while their kinetic energies E_B and E_y are respectively equal to

$$E_B = \frac{q^2}{2m_B} = \frac{m_{By}}{m_B} Q, \quad E_y = \frac{q^2}{2m_y} = \frac{m_{By}}{m_y} Q. \tag{2.4}$$

If the decay is virtual, i.e., if it occurs only for a finite time, then the energies of the particles E_B and E_y cannot be measured exactly, while the momenta, being variables canonically conjugate to the spatial coordinates, can have completely definite values at each instant of time. Therefore relations (2.4) do not exist (it is said that the particles B and y are "off the mass shell"):

$$E_B \neq \frac{q^2}{2m_B}, \quad E_y \neq \frac{q^2}{2m_y}, \tag{2.5}$$

while the laws of conservation of energy and momenta are valid as before in virtue of the homogeneity of space and time:

$$E_B + E_y = Q, \quad \mathbf{p}_B + \mathbf{p}_y = 0. \tag{2.6}$$

Thus, in this case we have two independent variables the values of which are not fixed by the conservation laws: the energy of one of the particles (E_B or E_y) and the square of the momentum q^2 in the center of mass system. The invariant amplitudes describing the virtual decay are functions of the variables indicated above. But the amplitudes for the real decay are numbers corresponding to the values of these functions at points determined by equations (2.3) and (2.4).

In an analogous manner one can introduce the amplitudes for other more complicated virtual processes. In particular, the simplest mechanism for the reaction

A(x, xy)B of quasielastic scattering of particle x by particle y reduces to two virtual processes: the decay $A \to B + y$ and the elastic scattering y(x, x)y (cf., Fig. 6). The invariant amplitudes for the process of scattering of real particles, as has been elucidated in the preceding section, are functions of two independent variables, for example, s_{xy} and t_{xx}. But if the particle y is virtual and as a result of this is off the mass shell, then the amplitude for the scattering process will also depend on one more variable $P_y^2 \neq m_y^2$ [1]. According to the conservation laws we have

$$P_y = P_A - P_B. \tag{2.7}$$

Therefore

$$P_y^2 = t_{AB}, \tag{2.8}$$

with, in contrast to the scattering of real particles, $t_{AB} \neq m_y^2$. Correspondingly in the nonrelativistic approximation we have

$$\bar{t}_{AB} = -\frac{m_A}{m_B} q^2. \tag{2.9}$$

In the case of real scattering q^2 satisfies Eq. (2.3), and then we have

$$\bar{t}_{AB} = -2m_y Q. \tag{2.10}$$

Equation (2.10) does not hold for virtual scattering.

Thus, the invariant amplitudes for elastic scattering will depend in the example under consideration on three variables s_{xy}, t_{xx} and t_{AB} (or $\bar{t}_{AB}$). Since the kinetic energy of the virtual particle y is negative if the target nucleus A is stable then the values of all three variables will, generally speaking, differ from those which are realized in the scattering of free particles. However, it is important to emphasize that both real and virtual scattering is described by the same analytic functions but only corresponding to different values of the invariant variables.

Amplitude of Quasielastic Scattering

We now determine the form of the amplitude for the reaction A(x, xy)B corresponding to the mechanism of quasielastic scattering described above. For simplicity we shall assume that all the particles are spinless, so that each of the two virtual processes will be described by one invariant amplitude.

We denote the amplitude for the virtual decay (2.1) by M_1, and the amplitude for the elastic scattering y(x, x)y by M_2. Then in accordance with (1.5) the probability of decay dW_1 during a small time Δt will be given by

$$dW_1 = \Delta t \frac{|M_1|^2}{(2\pi)^2} \frac{\Delta T}{2\pi} \delta(P_A - P_B - P_y)\, d^3p_B\, d^3p_y\, d\mathcal{E}_y. \tag{2.11}$$

The factor $\Delta T d\mathcal{E}_y/2\pi$ in (2.11), where ΔT is a macroscopic time large compared to the reaction time Δt, takes into account the increase in the dimensionality of the phase space as a result of the fact that the energy of the virtual particle $\mathcal{E}_y$ has become an independent degree of freedom. The probability dW_2 for elastic scattering will be given by

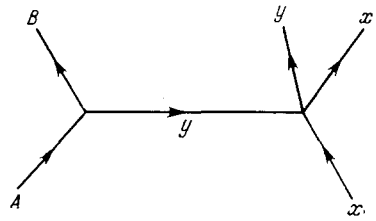

FIG. 6. Diagram for quasielastic scattering.

$$dW_2 = \Delta t \frac{|M_2|^2}{(2\pi)^2} \delta(P_y + P_x - P_y' - P_x')\, d^3p_x'\, d^3p_y'. \tag{2.12}$$

(Here the primed quantities refer to the final state.) The probability dW for the complete process as a whole will evidently be obtained by integrating the product $dW_1 dW_2$ over all the values of the energy and the momentum of the virtual particle y. Carrying out this integration we obtain

$$d\lambda = \frac{dW}{\Delta T} = |M_1 M_2\, \Delta t|^2 \delta(P_A + P_x - P_B - P_y' - P_x') \frac{d^3p_B\, d^3p_x'\, d^3p_y'}{(2\pi)^5}. \tag{2.13}$$

Comparing (2.13) with (1.5) we find that the desired amplitude M of the complete process as a whole is given up to a phase factor by the equation

$$M = M_1 M_2\, \Delta t. \tag{2.14}$$

In order to find Δt we can utilize the uncertainty relation

$$\Delta\mathcal{E}_y \cdot \Delta t = 1, \tag{2.15}$$

where $\Delta\mathcal{E}_y$ is the deviation of the energy of the virtual particle from the mass shell. Since Q is considerably smaller than m_y we can utilize the nonrelativistic relation between the energy and the momentum. Then we have

$$\Delta\mathcal{E}_y = E_y - \frac{p_y^2}{2m_y} = -\frac{p_y^2 - 2m_y E_y}{2m_y}. \tag{2.16}$$

Substituting (2.16) into (2.14) we obtain

$$M = -2m_y \frac{M_1 M_2}{p_y^2 - 2m_y E_y} = 2m_y \frac{M_1(\bar{t}_{AB})\, M_2(\bar{t}_{AB}, s_{xy}, t_{xx})}{\bar{t}_{AB} - 2m_y \varepsilon}, \tag{2.17}$$

where

$$\varepsilon = -Q = m_B + m_y - m_A \tag{2.18}$$

is the binding energy of the particle y to the nucleus B.

We now compare formula (2.17) with the diagram of Fig. 6. Utilizing the diagram we can easily write down the expression for the amplitude if we agree to make the vertices correspond to the amplitudes M_1 and M_2,

*By P_Y, P_A, P_B respectively we have denoted the four-momenta of particle y and of nuclei A and B.

and the internal line to the factor proportional to $2m_y/(p_y^2 - 2m_yE_y)$ which is called the propagator.

General Formula for the Amplitude Corresponding to a Feynman Diagram

The qualitative argument carried out above can be replaced by a more rigorous one based on utilizing the apparatus of second quantization. With its aid we can obtain the amplitudes for reactions involving a larger number of virtual particles and processes. Moreover, just as in the example of quasielastic scattering considered above the amplitude can be represented graphically by means of the following correspondence rules:

a) to each r-th vertex we set in correspondence the amplitude of the virtual process M_r:

b) integration over independent (i.e., not fixed by the conservation laws) four-momenta of the virtual particles corresponds to the element of phase volume $d^3kdE/(2\pi)^4$ ($\mathbf{k}$ is the momentum of the virtual particle, E is its kinetic energy);

c) to each internal line we set in correspondence the propagator

$$-\frac{2im}{k^2-2mE-i\eta},$$

where $\eta > 0$ is an infinitesimal increment which indicates the rule for going around the poles in the course of integration.

To this we should add that at each vertex the law of conservation of four-momentum holds, and that the common coefficient of the amplitude is the phase factor i^{v-1} where v is the number of vertices in the diagram (i.e., the number of virtual processes). If the diagram contains v vertices and n internal lines, then the number l of independent four-momenta of virtual particles is given by the relation

$$l = n - v + 1. \tag{2.19}$$

In accordance with what is stated above the amplitude for the process has the form

$$M = N\int \frac{M_1M_2 \dots M_v\, d^3k_1\, dE_1 \dots d^3k_l\, dE_l}{(k_1^2-2m_1E_1-i\eta)\dots(k_n^2-2m_nE_n-i\eta)}, \tag{2.20}$$

$$N = \frac{(-i)^l\, 2^{n-4l}}{\pi^l}\, m_1m_2 \dots m_n. \tag{2.21}$$

The expression (2.20) is also valid when the particles participating in the reaction have arbitrary spins. Only in this case the integral sign should be interpreted also as involving a summation over the components of the spins of the virtual particles.

The amplitude (2.20) has been written on the assumption that all the virtual particles are nonrelativistic, while the initial and final particles can have arbitrary energies. Just such a situation is realized in nuclear reactions (in particular, also at high energies) when the energy and the momentum transferred to the nucleus are small.

For one and the same reaction one can indicate an infinite number of Feynman diagrams. For example, for the reaction A(x, xy)B, in addition to the diagram of Fig. 6 there exists also a set of comparatively simple diagrams taking into account the interaction of the virtual particle y with the residual nucleus (Fig. 7). The mechanism corresponding to this diagram contains, compared with the diagram of Fig. 6, one more virtual reaction—scattering (elastic or inelastic) of the particle y by the nucleus B (with the inelastic scattering capable of occurring both with an increase or a decrease in the kinetic energy of the colliding particles y and B). Thus, generally speaking, the total amplitude for the reaction represents a sum of an infinite number of terms of the type (2.20). In the modern theory of nuclear reactions as a rule one takes into account one or several diagrams, and in the best case the sum of a selected infinite series of diagrams.

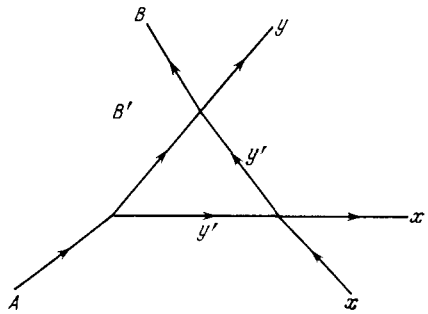

FIG. 7. Final state interaction.

One can indicate several considerations which to a greater or lesser extent justify the selection of diagrams usually carried out.

The first of these consists of the fact that the amplitudes for virtual reactions (for example, of the type of the decay of a nucleus into two particles) are different for different particles, and can be much larger for some of these than for others. In this case the representation of the amplitude for the reaction in the form of a series of Feynman diagrams will be similar to the series arising in perturbation theory but not in terms of the constant of strong interaction, but in terms of the effective values of the amplitudes for the virtual processes, and this is not the same thing.

A second important circumstance is that in order to explain the variation of the differential cross sections it is essential to separate out from the amplitude the most rapidly varying terms. A function varies most rapidly near its singular points. Therefore, the problem consists of picking out such diagrams the singularities of which are situated closest of all to the physical region. The singularities of the amplitude (2.20) can be determined on the one hand by the singularities of the amplitudes for the virtual processes, and on the other hand by the denominator of the integrand. The latter means that even in the case when the amplitudes for the virtual processes are constants

the integral (2.20) nevertheless represents a definite function of the invariant kinematic variables entirely determined by the mechanism of the process, i.e., by the number and by the type of the virtual particles and also by the sequence of the reactions in which they take part. Thus, the problem arises of finding the singularities of the integrals (2.20) and of selecting from them those nearest to the region in which a study of the differential cross section is being made. It is essential that these singularities can be found without evaluating the integral itself which is not always possible to perform analytically.

Singularities of the Diagrams

The rules for finding the singularities of Feynman diagrams were indicated in a general form by Landau[8] and have been developed with reference to nonrelativistic diagrams by Blokhintsev, Dolinskiĭ, and Popov[9-14] (cf., also[12]). These rules consist of the requirements that the values of the energies and the momenta of all the virtual particles at a singular point must:

a) satisfy the laws of conservation of four-momentum at each vertex of the diagram;

b) lie on the mass shell;

c) satisfy the "stretching" equation

$$\sum_{r=1}^{n} \alpha_r \lambda_r P_r = 0, \quad \sum_{r=1}^{n} \alpha_r = 1. \tag{2.22}$$

Here P_r are the four-momenta of the virtual particles, the summation is carried out over all the internal lines and λ_r is a sign factor equal to ± 1 depending on whether a given internal line is directed along or opposite to the positive direction of the closed circuit of the diagram (the choice of this direction is, naturally, arbitrary). From these rules it follows, in particular, that at a singular point the energies and momenta of all the virtual particles are determined uniquely. If the singularity of the diagram does not accidentally coincide with a singularity of some amplitude for the virtual processes then these amplitudes can be regarded as constants in the neighborhood of the singularity of the diagram and taken outside the integral sign in (2.20). This means that the variation of the differential cross section near a singularity of the Feynman diagram is determined directly and exclusively by the mechanism of the process. An experimental study of the cross sections in these domains of variation of the kinematic invariants is of the highest interest.

As we have already noted, the singularities of the Feynman diagrams with the exception of the normal thresholds with respect to the energy variables lie in the unphysical region. In connection with this it is always desirable to design an experiment in such a manner as to have the possibility to approach the singular point extremely closely. In this respect the use of high energy particles opens up, as can be seen from what follows (cf., Sec. V), a number of new possibilities.

The singular points of the amplitude (2.20) have a simple physical meaning: since at a singular point all the virtual particles are on the mass shell, then according to (2.15) this means that the duration of the existence of a virtual state, i.e., the duration of the reaction, is $\Delta t = \infty$. Thus, as we approach the singularity the duration of the reaction must increase.

The singularities of the Feynman diagrams are divided according to their nature into simple poles, and also into root and logarithmic branch points. The poles correspond to all the diagrams with a single internal line. Therefore, such diagrams are called pole diagrams. In particular, the diagram of Fig. 6 corresponds, as can be seen from (2.17), to a pole with respect to the variable $\bar{t}_{AB}$. Diagrams containing two or more internal lines correspond to branch points. In particular, the diagram of Fig. 7 corresponds to two branch points (a root and a logarithmic branch point) with respect to the variable s_{By} and to a logarithmic branch point with respect to the variable t_{xx}. We note a useful relation between the singularities of diagrams which can be converted into one another by condensing into a point a single or several lines: a given diagram contains within it all the singularities of the diagrams obtained by "condensing" it.

We point out two important consequences of the nonrelativistic approximation with respect to the virtual particles. The first of them consists of the fact that the amplitudes of the diagrams containing unidirectional closed circuits are equal to zero. One such diagram is shown in Fig. 8.

This rule is related to the fact that a nonrelativistic propagator contains in the denominator the first power of the energy, or, in other words, it has one pole and not two (corresponding to a particle and an antiparticle), as in the relativistic case.

The second consequence is also related to the choice of diagrams. It consists of the fact that only those diagrams must be utilized for which the numbers n and l satisfy the inequality

$$n > \frac{5l}{2}. \tag{2.23}$$

The inequality (2.23) guarantees the convergence of the

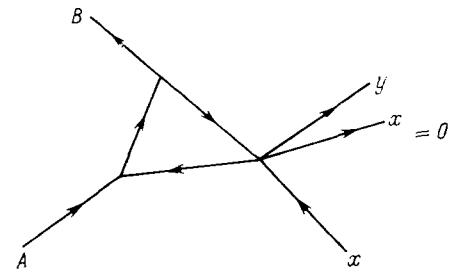

FIG. 8. Diagram with a unidirectional closed contour.

integrals (2.20) even in the case when all the amplitudes of the virtual processes can be regarded as constants. In this case the effective domain of integration is nonrelativistic: it is determined by the binding energies at the vertices or by the values of the nonrelativistic kinematic invariants. If the inequality (2.23) is not satisfied the convergence of the integral (2.20) can be due only to the falling off of the form factors contained in the amplitudes for the virtual processes. This falling off must be sufficiently rapid in order to make the effective domain of integration in (2.20) a nonrelativistic one. Since the remainder of the integrand at most does not fall off with an increase in the four-momenta of the virtual particles, it follows that the total integral as a whole will be small (of the order $\sqrt{\epsilon/m}$ or less) compared with the diagrams satisfying relation (2.23) (for greater details on this point see[4]).

The impulse approximation in the theory of reactions at high energies in fact reduces to an investigation of a pole (Fig. 6) and a triangular (Fig. 7) diagram. The amplitudes corresponding to these diagrams have different singularities and a number of other characteristic features which can be utilized in order to determine experimentally the relative contribution that each of them makes to the total amplitude for the reaction.

In subsequent sections we shall investigate the properties of the diagrams of Fig. 6 and 7 and we shall indicate certain experiments desirable from the theoretical point of view.

III. THE POLE APPROXIMATION

Domain of Applicability

The applicability of the pole approximation is restricted to small transferred momenta q. Specifically we must have

$$0 \leqslant q^2 \leqslant \varkappa^2, \tag{3.1}$$

where

$$\varkappa^2 = 2m_{By}\varepsilon. \tag{3.2}$$

The restriction (3.1) is associated with the fact that for large q^2 it becomes essential to take into account diagrams with singularities further removed from the physical region. The point is that as we move away from the singular point the rate of variation of the function and its absolute value cease to depend on the position of the singular point, and, therefore, for $q^2 \gg \kappa^2$ the diagram with the nearest pole singularity has no special features distinguishing it from the others. The inequality (3.1) is not, of course, a sufficient condition for the applicability of the pole approximation. It is hardly possible at the present time to give a literal formulation of such a condition. Therefore, it is extremely important to have a criterion with the aid of which one might experimentally establish the correctness of the pole approximation in each specific case.

The Treiman-Yang Criterion

The formula (2.17) for the pole diagram shown in Fig. 6 is distinguished by two notable properties: the amplitude of the reaction is first of all factorized, i.e., it can be separated into a product of two amplitudes and a propagator and, secondly, it depends only on the three variables, s_{xy}, t_{xx}, and t_{AB}, instead of five (cf., (1.19)) in the general case. The first of these properties enables us to express the differential cross section for the reaction in terms of the differential cross section for the virtual process at the right hand vertex (elastic scattering in the present case), while the second property enables us to indicate a simple, in principle, method for experimentally separating out the pole mechanism, which has been given the name of the Treiman-Yang criterion[13].

The essence of this criterion consists of the following. In the rest system of the incident particle x (i.e., in the system in which $\mathbf{p}_x = 0$) all three invariants s_{xy}, t_{xx}, and t_{AB} do not vary as the $(\mathbf{p}'_x, \mathbf{p}'_y)$ plane is rotated around the direction of the momentum of the virtual particle:

$$\mathbf{p}_y = \mathbf{p}_A - \mathbf{p}_B = \mathbf{p}'_x + \mathbf{p}'_y. \tag{3.3}$$

where $\mathbf{p}'_x$ and $\mathbf{p}'_y$ are the momenta of the final particles x and y. From this it follows that the corresponding differential cross section also will not vary under such a rotation.

In order to carry out a verification of the Treiman-Yang criterion it is necessary to vary the direction of emission of the final particles and the energy of one of them (if the energy of the incident particle is known). The relation between the differential cross section $d\sigma/d\Omega'_x d\Omega'_y d\mathcal{E}'_x$ measured in the laboratory reference system and the square of the modulus of the amplitude for the reaction can be easily obtained by utilizing formula (1.2):

$$|M|^2 = \frac{(2\pi)^5}{\mathcal{E}_B \mathcal{E}'_x} \frac{p_x}{\mathcal{E}_x} \frac{\left| \dfrac{\mathcal{E}'_x - \mathcal{E}_0}{\mathcal{E}'_x} p'_y - p'_x z'_{xy} + p_x z_{xy} \right|}{p'_x p'^2_y} \frac{d\sigma}{d\Omega'_x\, d\Omega'_y\, d\mathcal{E}'_x}. \tag{3.4}$$

Here $\mathcal{E}_0$ is the total energy of the colliding particles in the laboratory reference system, $d\Omega'_x$, $d\Omega'_y$ are the elements of the solid angles for the final particles

$$z_{xy} = \frac{\mathbf{p}_x \mathbf{p}'_y}{p_x p_y}, \quad z'_{xy} = \frac{\mathbf{p}'_x \mathbf{p}'_y}{p'_x p'_y}. \tag{3.5}$$

Formula (2.17) was obtained on the assumption that the spins of all the particles participating in the reaction are equal to zero. In this case we have

$$|M|^2 = \frac{|F|^2}{2^5 \mathcal{E}_A \mathcal{E}_B \mathcal{E}_x \mathcal{E}'_x \mathcal{E}'_y}, \tag{3.6}$$

where F depends exclusively on the invariant variables. Substituting (3.6) into (3.4) and taking into account the fact that in the laboratory system $\mathcal{E}_A = m_A$ we obtain the quantity $|F|^2$ which is invariant with respect to the Treiman-Yang rotation:

$$|F|^2 = 2^{10}\pi^5 \frac{\mathcal{E}'_y p_x}{p'_x p'^2_y} \frac{\mathcal{E}_0 - \mathcal{E}'_x}{\mathcal{E}'_y} p'_y + p'_x z'_{xy} - p_x z_{xy} \frac{d\sigma}{d\Omega'_x\, d\Omega'_y\, d\mathcal{E}'_x}. \tag{3.7}$$

The fact that the particles have spins is essential in two respects. Firstly, in this case the amplitudes of the virtual reactions depend not only on the invariant variables but also on the spin-tensors and the momenta of the particles. Secondly, in formula (2.17) one must carry out a summation over the components of the spin of the virtual particle.

It can be shown that for particles with spin expression (3.6), averaged and summed over the components of the spins of the initial and the final particles, which we denote by the symbol $\overline{|F|^2}$, also depends only on the invariant variables. It is clear that the applicability of the Treiman-Yang criterion in the case of particles with spin depends on the factorizability of the quantity $\overline{|F|^2}$. Indeed, if factorization occurs then this means that the virtual processes of decay and scattering can be regarded as independent. In this case noninvariance with respect to the Treiman-Yang rotation is equivalent to an azimuthal asymmetry of the scattering process in the system in which the incident particle x is at rest. Such asymmetry can occur only if at least one of the colliding particles is polarized. In the case under consideration the beam of x particles is not polarized. As regards the particles y, their source is the virtual decay of the nucleus A. But if the nucleus A is not polarized, and we do not observe a polarization of the nucleus B then the particle y also cannot be polarized, since in the center of mass system of the particles B and y there is no physically preferred plane.

If the spin J_y of the virtual particle y is equal to zero, then $\overline{|F|^2}$ will be invariant with respect to the Treiman-Yang rotation, since in this case the amplitude of the reaction is itself factorized. If $J_y \neq 0$, then, generally speaking, $\overline{|F|^2}$ is not factorized, but for nonrelativistic virtual particles one can indicate a fairly broad class of processes when factorization does occur[14]. In order to enumerate these cases we consider the spin characteristics of the virtual reactions appearing in the diagram of Fig. 6.

The decay A → B + y can be conveniently characterized by the spin of the exit channel J_{By} which takes on the values

$$|J_B - J_y| \leqslant J_{By} \leqslant J_B + J_y, \tag{3.8}$$

and by the number L_{By} restricted to the range

$$|J_A - J_{By}| \leqslant L_{By} \leqslant J_A + J_{By}. \tag{3.9}$$

The virtual scattering y(x, x)y can be described with the aid of the spins of the entrance (J_{xy}) and exit (J_{xy}) channels and by their vector difference L_{xy}. These quantities satisfy the inequalities

$$|J_x - J_y| \leqslant J_{xy}, \quad J'_{xy} \leqslant J_x + J_y, \tag{3.10}$$

$$|J_{xy} - J'_{xy}| \leqslant L_{xy} \leqslant J_{xy} + J'_{xy}. \tag{3.11}$$

In the case of nonrelativistic virtual particles factorization of $\overline{|F|^2}$ occurs if at least one of the following conditions is satisfied:

$$J_y = 0,\ 1/2, \tag{3.12}$$

$$J_{By} = 0,\ 1/2, \tag{3.13}$$

$$L_{By} = 0. \tag{3.14}$$

If all the particles participating in the reaction are nonrelativistic then invariance with respect to the Treiman-Yang rotation will also occur in two other cases:

$$J_{xy} = 0,\ 1/2, \tag{3.15}$$

$$L_{xy} = 0. \tag{3.16}$$

Everything stated above refers to the reaction A(x, xy)B. However, the results obtained above can be easily reformulated for any reaction of the type A(x, yz)B in which the virtual particle does not coincide with any of the final particles (cf.,[14]). In exactly the same manner one can obtain the conditions analogous to (3.12)—(3.16) for pole reactions with an arbitrary number of final particles[15].

The Treiman-Yang criterion is a necessary but not a sufficient characteristic of a pole mechanism. However, an investigation of triangular diagrams shows that invariance with respect to the Treiman-Yang rotation in this case requires that certain conditions should be satisfied which are rarely realized in practice. It should be emphasized that the Treiman-Yang criterion is the only method of establishing the pole mechanism which is independent of the specific form of the amplitudes for the virtual processes. Unfortunately, at the present time there are no published experimental papers utilizing this criterion for the identification of the pole mechanism of nuclear reactions.

We note that for reactions which do not satisfy conditions (3.10)—(3.16) the Treiman-Yang rotation can nevertheless be utilized to identify a pole mechanism, since in this case $\overline{|F|^2}$ is a polynomial of the r-th degree in cos φ, where φ is the angle of rotation, while the number r is defined by the inequality[17]

$$r = \min(2L_{By}, [J_{By}], [J_y], [J_{xy}], 2L_{xy}). \tag{3.17}$$

Here

$$[J] = \begin{cases} 2J, & \text{if J is integer,} \\ 2J-1, & \text{if J is half-integer.} \end{cases} \tag{3.18}$$

If the mechanism of the reaction is not a pole mechanism, then the dependence on cos φ will, generally speaking, not be a polynomial (cf.,[16]).

It should be noted that in certain recently published papers devoted to the Treiman-Yang criterion there are erroneous assertions regarding the applicability of this criterion in the case of relativistic virtual particles with spin ½ ([18,19]) and regarding the symmetry $\overline{|F|^2}_{\varphi=0} = \overline{|F|^2}_{\varphi=\pi}$[6] which allegedly holds for all pole

reactions (actually $\overline{|F|^2}$ contains both even and odd powers of cos φ; cf.,[17]).

Differential Cross Section in the Pole Approximation

If any one of the conditions (3.10)—(3.16) is satisfied, then the differential cross section for the reactions A(x, xy)B, averaged and summed over the components of the spins of the initial and final particles, can be expressed in terms of the differential cross section for elastic scattering y(x, x)y. In the laboratory reference system ($\mathbf{p}_A = 0$, $\mathcal{E}_A = m_A$) we have after averaging and summing over the spin components:

$$\frac{d\bar{\sigma}}{d\Omega_x' d\Omega_y' d\mathcal{E}_x'} = \frac{\overline{|M|^2}}{(2\pi)^5} \frac{\mathcal{E}_B \mathcal{E}_x' \mathcal{E}_x p_x' p_y'^2}{p_x} \left| \frac{\mathcal{E}_0 - \mathcal{E}_x'}{\mathcal{E}_y'} p_y' + p_x' z_{xy}' - p_x z_{xy} \right|^{-1}, \tag{3.19}$$

where

$$\overline{|M|^2} = \frac{4m_y^2 \overline{|M_1|^2}\,\overline{|M_2|^2}}{(p_y^2 - 2m_y E_y)^2}. \tag{3.20}$$

Picking out the energy factors in $\overline{|M_2|^2}$ we introduce the invariant quantity

$$\overline{|F_2|^2} = 2^4 \mathcal{E}_y \mathcal{E}_x \mathcal{E}_x' \mathcal{E}_y' \overline{|M_2|^2}. \tag{3.21}$$

This quantity is related in the following manner to the differential cross section for scattering in the center of mass system for the final particles x and y:

$$\frac{d\tilde{\sigma}_{xy}}{d\tilde{\Omega}} = \frac{\overline{|F_2|^2}}{256\pi^4} \left(\frac{\tilde{p}_x'}{\tilde{p}_x} \right) \frac{1}{s_{xy}}. \tag{3.22}$$

Here the quantities indicated by a tilde refer to the center of mass system for the final particles x and y, i.e.,

$$\tilde{\mathbf{p}}_x' + \tilde{\mathbf{p}}_y' = 0. \tag{3.23}$$

The momentum of the virtual particle $\mathbf{p}_y$ in the laboratory system satisfies the equation

$$\mathbf{p}_y = -\mathbf{p}_B = \mathbf{q}. \tag{3.24}$$

Since, moreover, in this system the virtual particle is not relativistic, we have

$$E_y = -E_B - \varepsilon = -\frac{q^2}{2m_B} - \mathcal{E}. \tag{3.25}$$

Utilizing the formulas given above we obtain

$$\overline{|M|^2} = 2^6 \pi^4 m_{By}^2 \frac{s_{xy} \tilde{p}_x}{\mathcal{E}_x \mathcal{E}_y \mathcal{E}_x' \mathcal{E}_y' \tilde{p}_x'} \frac{\overline{|M_1|^2}}{(q^2 + \varkappa^2)^2} \frac{d\tilde{\sigma}_{xy}}{d\tilde{\Omega}}. \tag{3.26}$$

The quantity $\overline{|M_1|^2}$ can be represented in the form

$$\overline{|M_1|^2} = \frac{2\pi^2 \varkappa}{m_{By}^2} \gamma^2 |f(q)|^2, \tag{3.27}$$

where f(q) is the form factor characterizing the momentum distribution of the virtual particles, and γ^2 is the constant determining the probability of their emission. Specifically, if the decay (2.1) is actually possible, then the decay constant λ is related to γ^2 by the formula[20]

$$\lambda = \gamma^2 Q, \quad Q = m_A - m_B - m_y. \tag{3.28}$$

One can also indicate the relation of γ^2 to the dimensionless reduced width θ^2 commonly utilized in nuclear spectroscopy:

$$\gamma^2 = \sum_{J_{By}, l} \gamma^2_{J_{By} l}, \quad \gamma^2_{J_{By} l} = \frac{6}{(\varkappa R)^3} \frac{\theta^2_{J_{By} l}}{|h_l(i\varkappa R)|^2}. \tag{3.29}$$

Here R is the channel radius, l is the orbital angular momentum of the relative motion, h_l is the spherical Hankel function of the first kind (or the singular solution of the Coulomb problem if the particles are charged).

Combining formulas (3.19), (3.26) and (3.27) we obtain

$$\frac{d\bar{\sigma}}{d\Omega_x' d\Omega_y' d\varepsilon_x'} = 4\pi\varkappa |\gamma|^2 \frac{m_B}{m_y} \frac{p_y'^2}{\mathcal{E}_y'} \frac{p_x'}{p_x} \frac{\tilde{p}_x}{\tilde{p}_x'} s_{xy} \frac{d\tilde{\sigma}_{xy}}{d\tilde{\Omega}} \frac{|f(q)|^2}{(q^2 + \varkappa^2)^2}. \tag{3.30}$$

We now consider in somewhat greater detail the quantities f(q) and $d\sigma_{xy}/d\tilde{\Omega}$ appearing in (3.30).

The Form Factor f(q)

This function is determined by the structure of the nucleus but to a lesser extent than is ordinarily assumed. As has been already pointed out at the beginning of this section, the domain of applicability of the pole approximation, and consequently of formula (3.30), is restricted to small transferred momenta. For light nuclei the domain determined by the inequality (3.1) almost coincides with the range

$$0 \leqslant q^2 \leqslant \frac{1}{R^2}. \tag{3.31}$$

The channel radius R is the minimum distance between the particles B and y starting with which their relative motion can be regarded as free, or determined exclusively by the Coulomb interaction if both particles are charged. In other words, R is the effective range of the nuclear interaction between the particles B and y. If r is the average distance between them, then from the uncertainty relation between the momentum and the coordinate it follows that the interval (3.31) corresponds to the range

$$r \geqslant R. \tag{3.32}$$

Thus, where the pole approximation is applicable for the light nuclei, the principal contribution to the form factor comes from the external region in which there is no nuclear interaction between the particles (more accurately, in which the energy of this interaction is small compared to the kinetic energy). The structure of the nucleus affects f(q) in the range (3.31) principally by determining the orbital angular momentum of the relative motion of B and y. If for small q the form factor is mainly determined by the wave function for the relative motion in the exterior region (3.32) then in the absence of the Coulomb interaction (or when it is not significant) it is not difficult to obtain the following expression:

$$f_l(q) = i\eta [\eta j_l(\xi) h_{l-1}(\eta) - \xi j_{l-1}(\xi) h_l(\eta)] \left(\frac{\gamma_l^2}{\gamma^2} \right)^{1/2}. \tag{3.33}$$

Here

$$\gamma_l^2 = \sum_{J_{By}} \gamma^2_{J_{By}l}, \tag{3.34}$$

$$\xi = qR, \quad \eta = i\varkappa R, \tag{3.35}$$

j_l and h_l are respectively the spherical Bessel and Hankel functions of the first kind, l is the orbital angular momentum of the relative motion of the particles B and y determined by their spins and by the laws of conservation of angular momentum and parity in the decay (2.1). If these latter considerations do not determine l uniquely then

$$|f(q)|^2 = \sum_l |f_l(q)|^2. \tag{3.36}$$

The structure of the nucleus affects the quantities γ_l^2/γ^2 and, thus, also the relative importance of the different l in the expression (3.36).

The form factor (3.33) can be said to be a Butler form factor, since together with the pole denominator $(q^2 + \kappa^2)$ it determines the angular distribution of the products of the reaction in the Butler theory of deuteron stripping or pick up (in these reactions the virtual particle y is a proton or a neutron). We note that for $l \geq 1$ the form factor (3.33) is equal to zero for $q = 0$ and behaves like $(qR)^l$ for small qR. Therefore, for $l \neq 0$ it can turn out that the form factor (3.33) is small in the region determined by the inequality (3.1). Then the pole approximation will be generally inapplicable. Another important circumstance is the fact that the function (3.33) oscillates and, consequently, the expression (3.36) has zeros for $q \geq 0$. It is clear that in the neighborhood of these zeros the pole approximation also ceases to be valid since the differential cross section (3.30) will here be small and the essential role will be played by contributions from other diagrams.

Failure to take into account the limitations enumerated above on the applicability of the pole approximation is encountered quite frequently (this is manifested in the attempts to describe by means of formula (3.30) the experimental data over the whole physical region of variation of the variable q). Another common error is the belief that the study of the reaction A(x, xy)B is capable of yielding information concerning the momentum distribution of "particle y inside the nucleus A." From what we have stated above it is clear that in the region where the pole approximation is applicable the details of the nuclear model have only a small effect on the distribution with respect to q determined by formula (3 30). At the same time the reaction of quasielastic scattering can be a source for obtaining information on the reduced widths of nuclear states. It is essential to emphasize that the values of the quantities γ_l^2 obtained in this manner must agree with data obtained from other direct reactions the Feynman diagrams for which contain the same virtual decay (2.1). In particular, the nucleon reduced widths obtained from the reaction A(x, xN)B and the stripping and pick-up reactions B(d, N)A, A(N, d)B must agree if, as we think at present, at small transferred momenta the reactions indicated above have a pole character. At the same time the channel radii R must also coincide.

Differential Cross Section for Virtual Elastic Scattering

The quantity $d\bar{\sigma}_{xy}/d\tilde{\Omega}$ which appears as a factor in formula (3.30) differs from the differential cross section for elastic scattering of free particles firstly by the fact that it depends on q^2, and not only on s_{xy} and t_{xx}. The second difference consists of the fact that the domains of the variables s_{xy} and t_{xx} which are realized in the scattering of free particles and in the reaction A(x, xy)B do not coincide.

The impulse approximation in the theory of nuclear reactions is usually taken to mean the pole formula (3.30) into which instead of the true value of $d\bar{\sigma}_{xy}/d\tilde{\Omega}$ one substitutes its value for the scattering of free particles. In this case the particle y lies on the mass shell, and this in accordance with (2.3) means that

$$q^2 = -\varkappa^2. \tag{3.37}$$

Thus, in the impulse approximation it is assumed that

$$\frac{d\bar{\sigma}_{xy}}{d\tilde{\Omega}}(q^2, s_{xy}, t_{xx}) \approx \frac{d\bar{\sigma}_{xy}}{d\tilde{\Omega}}(-\varkappa^2, s^0_{xy}, t^0_{xx}), \tag{3.38}$$

where s^0_{xy} and t^0_{xx} correspond to a certain point on the boundary of the physical region for elastic scattering of free particles[2)].

Equation (3.38) means that $d\bar{\sigma}_{xy}/d\tilde{\Omega}$ is considered to be a sufficiently slowly varying function of the variables q^2, s_{xy}, t_{xx}. Naturally, this occurs by no means always. A necessary condition for the validity of (3.38) is that the scattering amplitude should have no singularities close to the region under consideration with respect to all three variables. This means that the applicability of the impulse approximation depends on the scattering mechanism.

We consider some examples. Let the particles x and y be nucleons If the one meson exchange would p play the dominant role in nucleon scattering then $d\bar{\sigma}_{xy}/d\tilde{\Omega}$ would not depend at all on q^2 since the corresponding diagrams (cf., Fig. 9a) have no singularities with respect to P_y^2.

In actual fact the essential contribution to the am-

*We want to make it clear that for a given energy E_x of the particles x in the laboratory system the values of s_{xy} are different in the cases of quasielastic scattering and of the scattering of free particles. At the same time, however, s_{xy} always lies within the physical region for free scattering. The latter, generally speaking, does not hold for t_{xx} due to the departure of particle y from the mass shell.

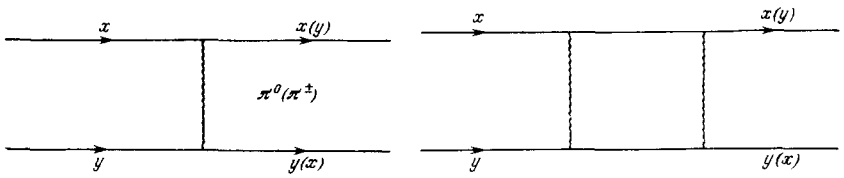

FIG. 9a. One meson exchange in nucleon-nucleon scattering.
FIG. 9b. Diagram for two meson exchange.

plitude is made by the many meson diagrams. One of the simplest of such diagrams is shown in Fig. 9b. This diagram has a singularity with respect to P_y^2 at the point

$$P_y^2 = (m + \mu)^2, \tag{3.39}$$

where m and μ are respectively the nucleon and the pion masses. Since

$$q^2 = -\frac{m_B}{m_A}(P_y^2 - m^2) - \varkappa^2, \quad \varkappa^2 \ll m^2, \tag{3.40}$$

Eq. (3.39) means that the nearest singularity of the amplitude for nucleon-nucleon scattering with respect to q^2 will occur at the point

$$q^2 = -2m_{By}\left[\mu\left(1+\frac{\mu}{2m}\right)+\varepsilon\right], \tag{3.41}$$

situated considerably further than the pole since $\mu/\epsilon \gtrsim 10$. Within the framework of the pole approximation taking into account such distant singularities of the amplitudes for virtual processes would mean going beyond the accuracy of the approximation. Therefore, in the case of quasielastic scattering of nucleons substitution into formula (3.30) of the value of $d\bar{\sigma}_{xy}/d\tilde{\Omega}$ on the mass shell appears to be justified. If the virtual particle y is a deuteron, a triton or an α-particle then, generally speaking, the situation becomes more complicated. An analysis of the simplest diagram shows, however, that in this case also over a definite range of values of the variables s_{xy} and t_{xx} going outside the mass shell turns out to be not significant.

The arguments given above are based on the assumption that the nearest singularities of the scattering amplitude with respect to the variable q^2 are determined by the simplest Feynman diagrams. This assertion, strictly speaking, until now has been proven neither theoretically nor experimentally. In this connection an experimental investigation of quasielastic scattering in order to obtain information concerning the quantity $d\bar{\sigma}_{xy}/d\tilde{\Omega}$ outside the mass shell appears to be particularly interesting.

The variation of $d\bar{\sigma}_{xy}/d\tilde{\Omega}$ in going from the point s_{xy} or t_{xx} in the physical region for the reaction A(x, xy)B to the point s_{xy}^0 or t_{xx}^0, lying in the physical region for the elastic scattering of free particles can be quite appreciable. Therefore, if formula (3.30) is used in order to study the properties of nuclei, i.e., for an experimental determination of the quantities γ^2, it is necessary to know the behaviour of $d\bar{\sigma}_{xy}/d\tilde{\Omega}$ as a function of the variables s_{xy} and t_{xx} in the physical region for the reaction A(x, xy)B. Unfortunately, such information is available only in rare cases. One such case is the elastic proton-proton scattering with respect to which it is known experimentally that for the scattering of free protons $d\bar{\sigma}_{xy}/d\tilde{\Omega}$ is practically independent of s_{xy} and t_{xx} over a comparatively broad range of energies of colliding particles from 150 to 430 MeV and is equal to 4 μb/sr (an exception is, of course, provided by the region of very small angles where the differential cross section is greater due to the usual Coulomb scattering). For this reason in the energy range indicated the reaction A(p, 2p)B is a good means to study the properties of nuclei.

One of the few cases when $d\bar{\sigma}_{xy}/d\tilde{\Omega}$ is known analytically is resonance scattering. Then within the limits of the width of the resonance the scattering cross section will be given by the Breit-Wigner formula. The broader the resonance, the greater will be the region within which the functional dependence of the scattering cross section on the kinematic variables is known. However, it is in this case essential that the resonance should be well pronounced (i.e., that the nonresonance part of the cross section should be sufficiently small). Such comparatively broad (of the order of 100 MeV) and at the same time sufficiently well pronounced resonances are encountered, for example, in the scattering of pions by nucleons.

IV. EXPERIMENTAL DATA AND THE POLE APPROXIMATION

The Reaction A(p, 2p)B

Reactions involving light nuclei are of the greatest interest since in this case the different states of the residual nucleus B are resolved.

The experiments discussed below have been so designed that final protons were recorded with equal momenta and emitted at equal angles θ with respect to the primary beam, with the momenta of all three protons (the initial one and the final ones) were coplanar (under these conditions a knowledge of the angle θ determines all the kinematic characteristics of the final particles).

Figure 10 shows the dependence of the differential cross section on the angle θ for the reaction $Li^6(p, 2p)He^{5*}$ (16.69 MeV) for an initial proton energy of 185 MeV in the laboratory reference system.

The ground state of Li^6 has spin and parity 1^+, while the state He^{5*} with an excitation energy of 16.69 MeV has spin and parity of $(3/2)^+$. Therefore, the orbital angular momentum l for the relative motion of He^{5*} and the virtual proton can have the values 0 and 2. The channel radius R = 5 F required for the calcula-

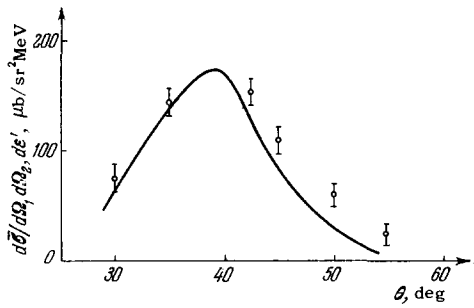

FIG. 10. Angular distribution of protons in the reaction $Li^6(p,2p)He^{5*}$(16.69 MeV). Solid curve – pole approximation.

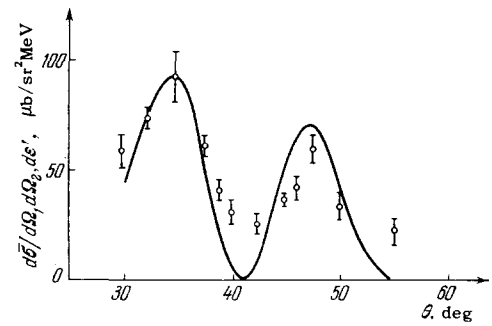

FIG. 12. Angular distribution of protons in the reaction $Li^7(p,2p)He^6$. Solid curve – pole approximation.

tion of the form factor has been taken from the experimental data on the pick-up reaction $Li^6(n, d)He^5$ [21], since the pole diagrams for this reaction and for the quasielastic scattering process contain the same vertex (cf., Fig. 11).

The solid curve in Fig. 10 has been calculated with the aid of formula (3.30) with the form factor (3.33) for $l = 0$ (all the theoretical calculations concerning the reaction A(p, 2p)B given below have been taken from the paper of Kolybasov and Smorodinskaya[22]). The differential cross section $d\bar{\sigma}_{pp}/d\tilde{\Omega}$ has been taken to be constant in agreement with what has been stated in the preceding section. The same diagram also shows the experimental data of Tibell and co- or workers[23]. The theoretical curve has been normalized to one of the experimental points.

Figure 12 shows the same dependence for the reaction $Li^7(p, 2p)He^6$ for a kinetic energy of the incident protons of 185 MeV. The ground state of Li^7 has spin and parity of $(3/2)^-$. The spins and parities of the ground and of the first excited (1.71 MeV) states of He^6 which were not resolved in the experiment under consideration are respectively equal to 0^+ and 2^+. In both cases $l = 1$. The channel radius is R = 5 F (from data on the reaction $Li^7(p, d)Li^6$). The results of a theoretical calculation[22] are shown in Fig. 12 by the solid curve, the experimental data have been taken from[23]. A characteristic feature of this diagram is the smaller depth of the experimental minimum compared to the theoretical one. As has already been noted previously this circumstance appears to be natural and is explained by the contribution of diagrams differing from the pole diagram.

We note that the range of angles $30° \leq \theta \leq 60°$ corresponds to relatively low transferred momenta q. For example, for the reaction $Li^7(p, 2p)He^6$ q lies in the interval $0 \leq q \leq 116$ MeV/c corresponding to the value $\kappa = 130$ MeV/c, so that the condition (3.1) for the applicability of the pole approximation is satisfied. As can be seen from Figs. 10 and 12 the agreement between theory and experiment in these cases can be regarded as satisfactory.

However, the picture is different when we go over to large transferred momenta. This is demonstrated by Fig. 13 which shows the experimental data from the work of Yuasa and Hourany[24] on the reaction $C^{12}(p, 2p)B^{11}$ for an initial proton energy of 90—110 MeV in the laboratory system. In this paper the differential cross section $d^2\bar{\sigma}/dqdz$ was measured where

$$z = -\frac{\mathbf{q}\mathbf{p}_x}{qp_x}. \tag{4.1}$$

For a given value of z the conservation laws limit the upper value of q which must satisfy the condition

$$\frac{E}{2} + \varepsilon - \frac{q^2(m+m_A)}{4mm_B} + \frac{pq}{2}z > 0, \tag{4.2}$$

where E and p are the kinetic energy and the momentum of the incident protons in the laboratory system.

The formula for the differential cross section within the framework of the pole approximation for nonrelativistic particles has the form

$$\frac{d\bar{\sigma}}{dq\,dz} = \text{const} \cdot \frac{|f(q)|^2}{(q^2+\varkappa^2)^2}\left[m\varepsilon + \frac{mE}{2} - \frac{q^2(m+m_A)}{4mm_B} + \frac{pq}{2}z\right]^{1/2}. \tag{4.3}$$

The solid curve in Fig. 13 is obtained by integrating

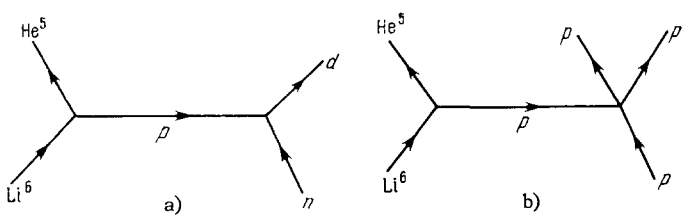

FIG. 11. Pole diagrams for the reactions: a) $Li^6(n,d)He^5$, b) $Li^6(p,2p)He^5$.

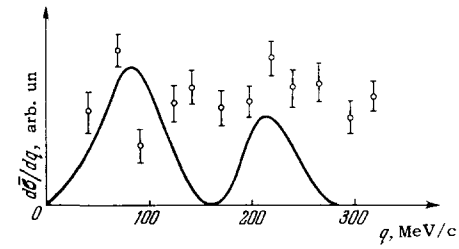

FIG. 13. Momentum spectrum of residual nuclei in the reaction $C^{12}(p,2p)B^{11}$. Solid curve – pole approximation.

over z within the range $0 \leq z \leq 1$. In carrying this out it was assumed that $l = 1$, R = 4.6 F on the basis of the data on the reaction $B^{11}(d, n)C^{12}$ [25]. The value of κ is in this case 166 MeV/c.

As can be seen from Fig. 13 one can speak of agreement between theory and experiment only for small transferred momenta $q \lesssim \kappa$. However, from a discrepancy between theory and experiment for $q > 200$ MeV/c it is not yet possible to conclude that the pole mechanism ceases to be dominant in this region (perhaps the Butler expression for the form factor is simply inapplicable in this region). At the same time there are also no grounds for assuming that the results shown in Fig. 13 give information on the momentum distribution of protons in the C^{12} nucleus. Such a conclusion could be made only after establishing the pole mechanism for the reaction under consideration preferably with the aid of the Treiman-Yang criterion which in this case is applicable (condition (3.12)). Not a bad method for establishing the correctness of the pole approximation is a comparison of the reduced proton widths obtained from the reaction A(p, 2p)B and from the stripping B(d, n)A or pick-up A(n, d)B processes. Such an analysis has been carried out in the paper by Kolybasov and Smorodinskaya[22] quoted above. Unfortunately the available experimental data are too unreliable and incomplete and, therefore, it is not possible as yet to make definite conclusions on their basis.

The Reaction $C^{12}(\pi^-, \pi^-n)C^{11}$

This process has been experimentally studied by Reeder and Markowitz[26] for an initial pion energy from 53 to 423 MeV. In the work quoted above, carried out by means of a radiochemical method, an investigation was made of the dependence of the total cross section on the initial energy, i.e., the excitation curve for the reaction was obtained. Although experimental information of this type is too all-inclusive and, in principle, is far from sufficient to establish the mechanism of the reaction, it is in the present case of interest because the range of energy of the incident pions utilized by the authors contains the resonant region corresponding to the nucleon isobar (3/2, 3/2) of mass 1236 MeV (to such a mass corresponds the resonance in the scattering of pions by free nucleons at a kinetic energy of 195 MeV in the laboratory system or at an energy of 157 MeV in the center of mass system). If the pole mechanism gives a significant contribution to the amplitude of the reaction under consideration then the (3/2, 3/2) resonance must show up in the excitation curve.

We have emphasized above that the pole approximation is valid for small momentum transfers. In the given case small momentum transfers were not specially picked out if we do not count the fact itself of the formation of the C^{11} nucleus in the ground or in weakly excited states (in the opposite case the nucleus would decay within a short time with the emission of nuclear particles and could not be recorded in terms of its beta activity). This circumstance should be taken into account since the probability of communicating to the nucleus a large amount of momentum without transferring energy to the internal degrees of freedom is small.

In accordance with the above considerations a comparison of the results of the pole approximation with the experimental data of Reeder and Markowitz[26] is of interest although, of course, it is hard to expect in this case anything more than qualitative agreement.

We have already indicated above that the existence of a broad and well pronounced resonance makes it easier to obtain a theoretical formula since the dependence of the Breit-Wigner scattering cross section on the variables s_{xy} and t_{xx} is known, and a departure of the virtual neutron off the mass shell appears in the first approximation to be without significance. The corresponding calculation has been carried out in[27], the results of which together with the experimental data[26] are given in Fig. 14. In this diagram the energy of the initial pion in the laboratory system has been plotted along the horizontal axis, and the total cross section for the reaction along the vertical axis. The solid curve represents the result of integrating the differential cross section (3.30) over the kinematic variables of the final particles. The Breit-Wigner formula was used here for the elastic scattering cross section $d\bar{\sigma}_{xy}/d\tilde{\Omega}$. The calculation was carried out on the assumption that the C^{11} nucleus is formed as a result of the reaction in its ground state. Actually, as is shown by an experimental study of the reaction $C^{12}(p, d)C^{11}$, the reduced neutron widths corresponding to the formation of C^{11} in the ground state $(3/2)^-$ and the three nearest excited states $(1/2^-, (3/2)^-, ?^-)$ are comparable. Nevertheless, taking into account the excited states of C^{11} does not appreciably alter the form of the solid curve in Fig. 14 (the excitation energies are not great and in all cases $l = 1$). In calculating the theoretical curve shown in Fig. 14, the only unknown quantity is the effective value of γ^2 or the reduced neutron width θ^2 associated with it. If the prin-

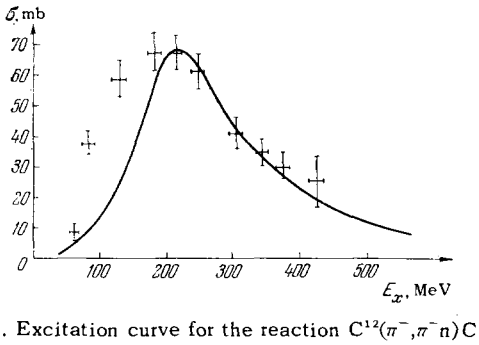

FIG. 14. Excitation curve for the reaction $C^{12}(\pi^-, \pi^-n)C^{11}$. Solid curve – pole approximation.

cipal contribution to the amplitude of the reaction is given by the pole diagram, then the reduced neutron widths θ^2 obtained from the data on the absolute values of the cross sections for the processes

$$C^{12}(\pi^-, \pi^- n) C^{11} \text{ and } C^{12}(p, d) C^{11},$$

must coincide. Assuming that the relative probability of formation of the C^{11} nucleus in the excited states is the same and is equal to approximately 0.7 (this number is known from experiments on the pick-up reaction) one can obtain from the quasielastic scattering cross section the following value for the reduced neutron width corresponding to the formation of C^{11} in its ground state:

$$\theta^2 = 0.38 \pm 0.07. \quad (4.4)$$

The error shown here is made up of the experimental errors in measuring the inelastic scattering cross section (the value at the maximum of the curve in Fig. 14 was utilized) and of the relative probability of the formation of C^{11} in the excited states. The value of θ^2 obtained from the pick-up reaction turns out to agree with (4.4) within the limits of error. Specifically, according to the data of[28] we have

$$\theta^2 \approx 0.34. \quad (4.5)$$

These results provide evidence in favor of the dominant role of the pole mechanism, although for final conclusions experiments are required on the measurement of the differential cross section and, in particular, the performance of a check by means of the Treiman-Yang criterion.

Experimental Problems of the Near Future

As can be seen from the preceding discussion, at the present time there does not in fact exist a sufficiently complete experimental proof of the dominant contribution of the pole diagrams to the mechanism of reactions of the type A(x, xy)B for small q. One can say that only the first steps have been taken in the experimental investigation of the role and of the domain of applicability of the pole approximation.

In this connection it is useful to formulate some experiments desirable from the theoretical point of view. Such experiments include:

1. The realization of the Treiman-Yang criterion for the reaction A(x, xN)B for different values of the transferred momenta q.

2. The measurement of the variation of the differential cross section $d\bar{\sigma}/dq$ as a function of q with a mandatory identification of the state of the residual nucleus.

3. The measurement of the absolute values of the differential cross sections for the reactions A(p, 2p)B and A(π, πN)B for small transferred momenta q and suitable energies of the initial particles (100—400 MeV for the reaction A(p, 2p)B and in the neighborhood of the πN resonances for the processes A(π, πN)B). The identification of the states of the residual nucleus B is also necessary in this case.

An important point in the carrying out the program indicated above is the realization of a complex investigation, i.e., the accumulation of data according to Secs. 1—3 for the same reaction.

V. FINAL STATE INTERACTION AND MOVING SINGULARITIES

Triangular Diagram

The pole mechanism yields singularities with respect to q^2, but there are no singularities with respect to the variables s_{xy} and t_{xx} due to the diagram itself. The simplest mechanism leading to the appearance of such singularities corresponds to the triangular diagram shown in Fig. 7. The whole process A(x, xy)B in this case reduces to three virtual reactions: the decay of the nucleus A into virtual particles B′ and y′

$$A \to B' + y', \quad (5.1)$$

the elastic scattering of the incident particle x by the virtual particle

$$x + y' \to x + y' \quad (5.2)$$

and the reaction leading to the production of the final particles B and y:

$$B' + y' \to B + y. \quad (5.3)$$

We denote the amplitudes for the reactions (5.1)—(5.3) respectively by M_1, M_2, and M_3. Then in accordance with the general formulas (2.20) and (2.21) the expression for the amplitude of the process A(x, xy)B corresponding to the triangular diagram of Fig. 7 will have the form

$$M_\Delta = -i\frac{m_y^2 m_{B'}}{2\pi^4} \times \int \frac{M_1 M_2 M_3\, d^3k_{y'}\, dE_{y'}}{(k_{y'}^2 - 2m_{y'}E_{y'} - i\eta)(k_{y'}^2 - 2m_{y'}E_{y'}' - i\eta)(k_{B'}^2 - 2m_{B'}E_{B'} - i\eta)}. \quad (5.4)$$

Here $k_{y'}'$ and $E_{y'}'$ are the momentum and the energy of the virtual particle y′ after scattering (5.2), the integral sign also includes summation over the components of the spins of the virtual particles.

Each of the amplitudes M_1, M_2, and M_3 depends on the kinematic variables of the virtual particles. However, since we are interested in the behavior of the amplitude M near the singularity we can assume M_1, M_2, and M_3 to be constants (cf., Sec. II). In this approximation the integral can be evaluated. In future we shall find it convenient to use in place of the variables s_{By} and t_{xx} the dimensionless variables ζ and λ defined in the following manner. Let E be the kinetic energy of the final particles B and y in their center of mass system, and Q be the energy liberated in the virtual reaction (5.3):

$$Q = m_{B'} + m_{y'} - m_B - m_y. \quad (5.5)$$

Then we have

$$\zeta = \frac{E-Q}{\varepsilon}, \tag{5.6}$$

where

$$\varepsilon = m_{B'} + m_{y'} - m_A. \tag{5.7}$$

The variable λ is related to the momentum $\mathbf{k}$ transferred in the scattering process (5.2):

$$\mathbf{k} = \mathbf{p}'_x - \mathbf{p}_x, \tag{5.8}$$

$$\lambda = \frac{m_{B'}^2}{m_A^2}\frac{k^2}{\varkappa^2}, \tag{5.9}$$

$$\varkappa^2 = 2m_{B'y'}\mathcal{E}. \tag{5.10}$$

In terms of the variables ζ and λ, the expression for the amplitude of the reaction has the form

$$M_\Delta = Cf_\Delta(\zeta, \lambda), \tag{5.11}$$

where the factor C depends on the components of the spins of the initial and the final particles, and

$$f_\Delta(\zeta, \lambda) = \frac{1}{\sqrt{\lambda}}\left[\frac{1}{2}\ln\frac{(\sqrt{\zeta}-\sqrt{\lambda})^2+1}{(\sqrt{\zeta}+\sqrt{\lambda})^2+1} + i\operatorname{arctg}\frac{2\sqrt{\lambda}}{\zeta-\lambda+1}\right], \quad \zeta \geqslant 0. \tag{5.12}$$

$$f_\Delta(\zeta, \lambda) = \frac{2i}{\sqrt{\lambda}}\operatorname{arctg}\frac{\sqrt{\lambda}}{1+\sqrt{-\zeta}}, \quad \zeta < 0, \tag{5.13}$$

with

$$0 < \operatorname{arctg} X < \pi. \tag{5.14}$$

The function f_Δ has two singularities: a root branch point

$$\zeta_0 = 0 \tag{5.15}$$

(the so-called normal threshold) and a logarithmic singularity ζ_Δ the position of which depends on the value of the transferred momentum k^2, i.e., on the variable λ:

$$\zeta_\Delta = \lambda - 1 + 2i\sqrt{\lambda}, \quad \lambda > 0. \tag{5.16}$$

If we regard f_Δ as a function of λ, then with respect to this variable there exists only one singularity—the logarithmic branch point

$$\lambda_\Delta = \zeta - 1 + 2i\sqrt{\zeta}. \tag{5.17}$$

In addition to the triangular diagram other diagrams (in particular the pole diagram discussed earlier) also give contributions to the amplitude of the reaction A(x, xy)B. Therefore, the total amplitude for the reaction M should be written in the form

$$M = M_\Delta + M_R, \tag{5.18}$$

where M_R denotes the contribution of all the other diagrams. Regarding the relative magnitude of $|M_\Delta|$ and $|M_R|$ it is, as a rule, difficult to make a definite theoretical statement, but the picking out of the amplitude M_Δ near ζ_Δ can be carried out experimentally, based on the fact that in this region M_R must vary considerably more slowly than M_Δ and, therefore, it can be treated as a constant.

The differential cross section averaged and summed over the components of the spins of the initial and the final particles can be written in the form

$$\frac{\partial^2\bar{\sigma}}{\partial\zeta\, d\lambda} = N\sqrt{\zeta}\,|f(\zeta, \lambda)|^2, \tag{5.19}$$

where N is a constant independent of ζ and λ (under the condition $\zeta \ll m_{By'}/\mathcal{E}$, $\lambda \ll m_x^2/x^2$),

$$|f(\zeta, \lambda)|^2 = |f_\Delta|^2 + 2a\,\mathrm{Re}\,f_\Delta + 2b\,\mathrm{Im}\,f_\Delta + c^2, \tag{5.20}$$

a, b, and c^2 are real constants. If the amplitudes M_Δ and M_R do not depend on the orientation of the spins of the particles participating in the reaction, then the number of independent constants is equal to two (in this case $c^2 = a^2 + b^2$).

Observation of the Complex Singularity

The constants a, b, and c^2 must be determined from the experimental data on the value of the differential cross section at three arbitrary points of the (ζ, λ) plane, and the surface so obtained must then describe the whole surface $\partial^2\bar{\sigma}/\partial\zeta d\lambda$ (we emphasize that this means a description with the aid of not more than three parameters of all possible curves corresponding to the different sections of the surface). In order to visualize the degree of sharpness of the dependences determined by formula (5.20) it is useful to construct for each of the first three terms in (5.20) contour lines (horizontals), i.e., curves in the (ζ, λ) plane along which the corresponding function of ζ and λ remains constant. The contour lines of the surfaces $|f_\Delta|^2$ and Re f_Δ are shown respectively in Figs. 15 and 16 taken from[29].

The surface Im f_Δ is very close in its structure to the surface $|f_\Delta|$ (this is related to the fact that in the domain of values of ζ, λ under consideration the principal contribution to $|f_\Delta|$ is made by Im f_Δ). From Figs. 15 and 16 it can be seen that in order to discover

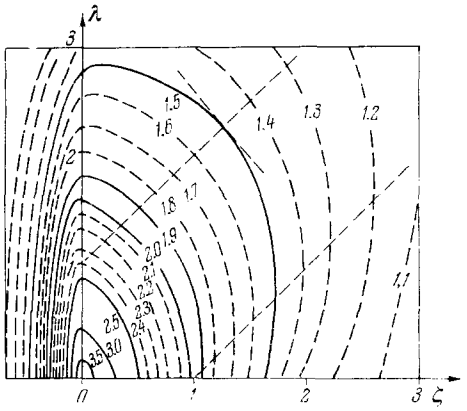

FIG. 15. Contour map of the surface $|f_\Delta(\zeta,\lambda)|^2$.

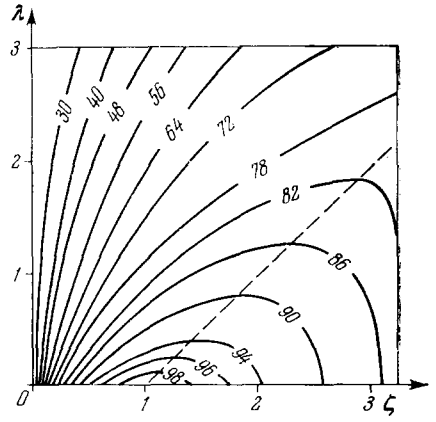

FIG. 16. Contour map of the surface Re $f_\Delta(\zeta,\lambda)$. (The numbers labelling the contour lines are equal to 100 Re f_Δ.)

dependences due to the complex singularity the sections by the planes λ = const or ζ = const are by no means always the optimal ones. In particular, if the dominant contribution to (5.20) is made by the terms $|f_\Delta|^2 + 2b\ \mathrm{Im}\ f_\Delta$, then the most prominent irregularity will manifest itself in taking the section by the vertical plane along the line orthogonal to the line

$$\lambda \quad \zeta \quad 1. \tag{5.21}$$

which is the projection of the trajectory (5.16) of the complex singularity ζ_Δ on the (ζ, λ) plane. But if the dominant contribution is made by the term 2a Re f_Δ then the most rapid variation will be exhibited by the curve obtained by taking the section by the vertical plane along the straight line orthogonal to the projection of the trajectory (5.17) of the complex singularity λ_Δ:

$$\zeta \quad \lambda \quad 1. \tag{5.22}$$

The dependence of the differential cross section on the kinematic variables k^2 and E will be the sharper the smaller are κ^2 and $\mathscr{E}$. This circumstance is a consequence of the approach of the complex singularity k^2_Δ or E_Δ to the (k^2, E) plane which contains the physical region.

Another important factor facilitating the experimental discovery of the complex singularity is the greatest possible size of the physical region. The size increases as the kinetic energy of the initial particle is increased. In particular, for

$$\sqrt{s_{Ax}} - m_A - m_x \quad , \tag{5.23}$$

the domain of the most rapid variation of Re f_Δ becomes accessible, while for

$$\sqrt{s_{Ax}} - m_A - m_x \quad \frac{(\alpha\mathscr{E} \quad \mathscr{E} \quad Q)^2}{4\alpha\mathscr{E}}, \qquad \alpha \quad \frac{m_B m_q}{m_{Bq}^2} \tag{5.24}$$

a segment of the straight line (5.21) falls in the physical region. We note that since for the majority of nuclei ϵ does not exceed 10 MeV kinetic energies of the order of 100 MeV in the center of mass system for the reaction are already sufficient for the experimental detection of the complex singularity corresponding to the diagram of Fig. 7.

Observation of a "Cusp"

We now investigate the manner in which the existence of a root singularity (5.15) affects the behavior of the cross section. This point lies within the physical region only in the case when $Q \geq 0$, i.e., when the virtual reaction (5.3) is exothermic, or when it is elastic scattering. An example of an exothermic virtual reaction (5.3) can be provided by the process of inelastic scattering with the "quenching" of an excitation, i.e., the case when the virtual particle B′ (or y′) is an excited state of the residual nucleus B (or y).

In the range

$$-\frac{Q}{\mathscr{E}} \leqslant \zeta \leqslant 0 \tag{5.25}$$

the expression for f_Δ is determined by formula (5.13). As can be easily seen comparing (5.12) and (5.13), f_Δ is continuous at the point $\zeta = 0$, while its first derivative undergoes a discontinuity at this point:

$$f'_\Delta(\zeta \to +0) \quad -\frac{1}{1-\lambda}\left[\frac{1}{1-\zeta} \quad \frac{2i}{1-\lambda}\right], \tag{5.26}$$

$$f'_\Delta(\zeta \to -0) \quad \frac{i}{(1-\lambda)\sqrt{-\zeta}}. \tag{5.27}$$

The discontinuity in the derivative will manifest itself in the differential cross section in the form of a characteristic peak—a "cusp"[30] (cf. also[31]), which will be the sharper the smaller is λ. Equations (5.26) and (5.27) show how the shape of the peak will vary as the transferred momentum varies. The curves corresponding to sections of the surfaces Im f_Δ and Re f_Δ by the vertical planes λ = const, are shown in Figs. 17 and 18.

The Reaction d(p, p)X

At the present time there exists not a single reliably established case of observing a moving complex singularity corresponding to a triangular diagram. However, several reactions are known which are "suspicious" in this respect. Thus, Valuev[32] and

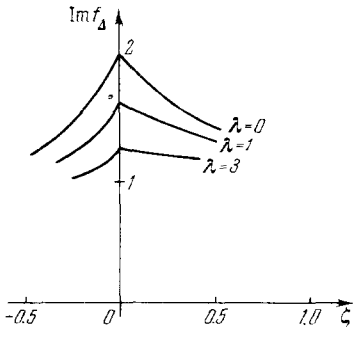

FIG. 17. Sections of the surface Im $f_\Delta(\zeta,\lambda)$ by the vertical planes λ = const.

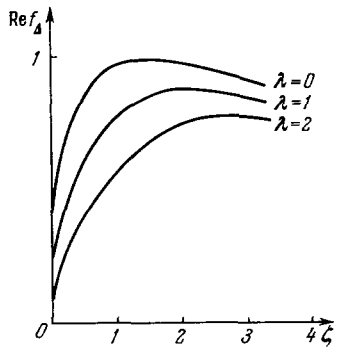

FIG. 18. Sections of the surface Re $f_\Delta(\zeta,\lambda)$ by the vertical planes λ = const.

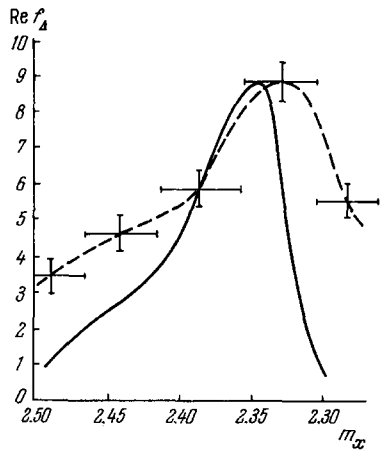

FIG. 19. The missing mass spectrum in the reaction p + d → p + X. Solid curve – triangular diagram.

independently Anisovich and Dakhno[33] have shown that experimental data on the reaction N(π, 2π)N which have been previously interpreted as proof of the existence of a two pion ABC-resonance can be explained by a singularity of the triangular diagram. An example of the same type belonging to the domain of nuclear reactions has been investigated by Dal'karov[34] who has theoretically investigated the reaction

$$p+d\to p+X. \tag{5.28}$$

Here the letter X denotes a combination of particles with total baryon charge 2 which were not recorded in the experiment carried out by Belletini and coworkers[35]. These authors had established the existence of a well pronounced maximum of width approximately 250 MeV in the missing mass spectrum for m_X, i.e., in the dependence of the differential cross section on the variable

$$\sqrt{s_x}=\sqrt{P_x^2}=[(P_p+P_d-P_p')^2]^{1/2}, \tag{5.29}$$

which, as can be easily seen, coincides with the variable $\sqrt{s_{By}}$ which appeared in the preceding investigation. This experiment was carried out with small transferred momenta k. In particular

$$10^{-3}<t_{pp}\,(\mathrm{GeV/c})^2<10^{-1}. \tag{5.30}$$

Fig. 19 shows experimental data obtained in[35] for $t_{pp} = 10^{-2} \times (\mathrm{GeV/c})^2$ (the dotted curve has been drawn through the experimental points). The solid curve represents the result of a theoretical calculation for Re f_Δ for the triangular diagram shown in Fig. 20.

According to this diagram the mechanism of the reaction under consideration consists of the fact that the incident proton on colliding with one of the nucleons of the deuteron forms the isobar N* which is subsequently inelastically scattered by the other nucleon. The solid curve in Fig. 19 is obtained on the assumption that N* is the isobar of mass (1.40 ± 0.01) GeV and of width Γ = 200 MeV (this isobar was observed by the same group of experimenters in the reaction p + p → p + N* and the maximum corresponding to it in the missing mass spectrum for small t_{pp} was more pronounced than other isobar peaks). We also note that in the theoretical calculation shown by the solid curve in Fig. 19 the amplitude for the virtual decay d → p + n was not treated as a constant—the form factor for the deuteron determined by the non-zero range of nuclear forces between nucleons was taken into account. However, taking this correction into account does not alter the principal result.

As can be seen from Fig. 19, the mechanism corresponding to the triangular diagram of Fig. 20 can indeed explain the observed experimental maximum. However, the same maximum can also be explained by a different hypothesis, viz., by the existence of a two-nucleon resonance of mass (2.33 ± 0.01) GeV. The choice between the two indicated possibilities must be made with the aid of further experiments: in the case of the mechanism corresponding to the triangular diagram the maximum of the curve of Fig. 19 will shift as t_{pp} is varied, but if the hypothesis regarding the two-nucleon resonance is valid then the position of the maximum will not depend on the values of this variable (we note that the accuracy of the data contained in[35] obtained for different values of t_{pp} is insufficient to answer this question).

VI. CONCLUDING REMARKS

In conclusion we consider the relation between the approximations utilized above and the well known results of Watson[36] and Migdal[37] on taking the final state interaction into account.

As has already been noted above, the starting point of our investigation was the assumption concerning nearness to the singularity and the relatively slow variation at this point of the amplitudes for the virtual processes. Watson and Migdal, on the contrary, consider the case when the dependence of the amplitude on the kinematic variables determined by the mechanism of the process itself is weak compared to the de-

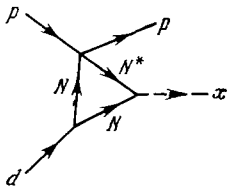

FIG. 20. Triangular diagram for the reaction d(p,p)X.

pendence of the amplitude for the virtual reaction (5.3) on the variable E.

From the whole above discussion one can conclude that the prospects of identifying the mechanism of the reaction and, in particular, of elucidating the role of the so-called final state interaction by means of an experimental observation of a moving logarithmic and root branch point of the amplitude corresponding to the triangular diagram appear to be quite realistic for a sufficiently high energy of the incident particles. At the present time only the first tentative steps have been taken in this direction.

[1] V. M. Kolybasov, YaF 3, 729 (1966), Soviet JNP 3, 535 (1966).

[2] A. O. Vaĭsenberg, É. D. Kalganova, and N. V. Rabin, JETP 47, 1962 (1964), Soviet Phys. JETP 20, 1318 (1965); Phys. Letters 2, 110 (1962).

[3] I. S. Shapiro, Proc. Int. Conf. on Nucl. Phys. 1, 313—319, Paris, 1964.

[4] S. Ozaki, R. Weinstein, G. Glass, E. Loh, L. Neimala, and A. Wattenberg, Phys. Rev. Letters 4, 533 (1960).

[5] T. Ericson, Proc. Int. Conf. on High Energy Phys. and Nucl. Structure, CERN, 1963, p. 47.

[6] D. H. Wilkinson, Proc. Phys. Soc. 80, 997 (1962).

[7] V. M. Kolybasov, YaF 3, 965 (1966), Soviet JNP 3, 704 (1966).

[8] L. D. Landau, Nucl. Phys. 15, 261 (1960).

[9] L. D. Blokhintsev, É. I. Dolinskiĭ, and V. S. Popov, JETP 42, 1636 (1962), Soviet Phys. JETP 15, 1136 (1962).

[10] L. D. Blokhintsev, É. I. Dolinskiĭ, and V. S. Popov, JETP 43, 2291 (1962), Soviet Phys. JETP 16, 1619 (1963).

[11] L. D. Blokhintsev, É. I. Dolinskiĭ, and V. S. Popov, JETP 43, 1914 (1962), Soviet Phys. JETP 16, 1350 (1963).

[12] I. S. Shapiro, Teoriya pryamykh yadernykh reaktsiĭ (Theory of Direct Nuclear Reactions) Moscow, Gosatomizdat (1963); "Selected Topics in Nuclear Theory," pp. 85—154, Vienna, 1963.

[13] S. B. Treiman and C. N. Yang, Phys. Rev. Letters 8, 140 (1962).

[14] I. S. Shapiro, V. M. Kolybasov, and I. P. Ayrem, Nucl. Phys. 61, 353 (1965).

[15] V. M. Kolybasov, Nucl. Phys. 68, 8 (1965).

[16] V. M. Kolybasov, ITEF (inst. of Theoret. and Exp. Phys.) Preprint No. 425 (1966).

[17] I. S. Shapiro and V. M. Kolybasov, JETP Letters 4, 329 (1966), transl. p. 221.

[18] L. J. Gutay, J. E. Lanutti, P. L. Csonka, M. J. Moravcsik, and M. D. Scadron, Phys. Letters 16, 343 (1965).

[19] C. Zemach, Phys. Rev. 140B, 109 (1965).

[20] I. S. Shapiro and S. F. Timashev, YaF 2, 445 (1965), Soviet JNP 2, 319 (1965).

[21] P. Tomas, G. Paic, V. Valcovic, M. Cerineo, J. Slans, and D. Rendic, Proc. Int. Conf. on Nucl. Phys. 2, 955, Paris, 1964.

[22] V. M. Kolybasov and N. Ya. Smorodinskaya, YaF 5, 777 (1967), Soviet Phys. JNP 5, 550 (1967).

[23] G. Tibell, O. Sundberg and P. Renberg, Arkiv Fysik 25, 433 (1964).

[24] T. Yuasa and E. Hourany, Phys. Letters 18, 146 (1965).

[25] E. E. Maslin, J. E. Price, and J. R. Risser, Nucl. Phys. 71, 433 (1965).

[26] P. L. Reeder and S. S. Markowitz, Phys. Rev. 133 B639 (1964).

[27] V. M. Kolybasov, YaF 2, 144 (1965), Soviet JNP 2, 101 (1965).

[28] D. Bachelier et al., Direct Interactions and Nuclear Reaction Mechanisms, p. 1141, Gordon and Breach Publ. N. Y.-London, 1963.

[29] É. I. Dubovoĭ and I. S. Shapiro, JETP 51, 1251 (1966), Soviet Phys. JETP 24, 839 (1967).

[30] A. I. Bas', JETP 33, 923 (1957), Soviet Phys. JET 6, 709 (1958).

[31] L. D. Landau and E. M. Lifshitz, Kvantovaya mekhanika (Quantum Mechanics), Moscow, Fizmatgiz, 196 p. 653.

[32] B. N. Valuev, JETP 47, 649 (1964), Soviet Phys. JETP 20, 433 (1965).

[33] V. V. Anisovich and A. G. Dakhno, JETP 46, 1152 (1964), Soviet Phys. JETP 19, 779 (1964).

[34] O. D. Dal'karov, JETP Letters 3, 150 (1966), transl. p. 94.

[35] G. Belletini, G. Cocconi, R. A. Diddens et al., Phys. Letters 18, 167 (1965).

[36] K. M. Watson, Phys. Rev. 88, 1163 (1952).

[37] A. B. Migdal, JETP 28, 3 (1955), Soviet Phys. JETP 1, 2 (1955).

Translated by G. Volkoff